International Journal of Earth Sciences (2022) 111:767–788
https://doi.org/10.1007/s00531-021-02146-1

ORIGINAL PAPER

Implications for sedimentary transport processes in southwestern Africa: a combined zircon morphology and age study including extensive geochronology databases

Andreas Gärtner[1] · Mandy Hofmann[1] · Johannes Zieger[1] · Anja Sagawe[1] · Rita Krause[1] · Marika Stutzriemer[2] · Subani Gesang[2] · Axel Gerdes[3,4] · Linda Marko[3,4] · Cristiano Lana[5,6] · Ulf Linnemann[1]

Received: 15 July 2021 / Accepted: 30 November 2021 / Published online: 17 December 2021

Abstract

Extensive morphological and age studies on more than 4600 detrital zircon grains recovered from modern sands of Namibia reveal complex mechanisms of sediment transport. These data are further supplemented by a zircon age database containing more than 100,000 single grain analyses from the entire southern Africa and allow for hypothesising of a large Southern Namibian Sediment Vortex located between the Damara Orogen and the Orange River in southern Namibia. The results of this study also allow assuming a modified model of the Orange River sand highway, whose origin is likely located further south than previously expected. Moreover, studied samples from other parts of Namibia give first insights into sediment movements towards the interior of the continent and highlight the potential impact of very little spatial variations of erosion rates. Finally, this study points out the huge potential of detrital zircon morphology and large geo-databases as an easy-to-use additional tool for provenance analysis.

Keywords Namibia · Zircon · Mineral morphology · Sediment transport · Geochronology · Database

✉ Andreas Gärtner
andreas.gaertner@senckenberg.de

Mandy Hofmann
mandy.hofmann@senckenberg.de

Johannes Zieger
johannes.zieger@senckenberg.de

Anja Sagawe
anja.sagawe@senckenberg.de

Rita Krause
rita.krause@senckenberg.de

Marika Stutzriemer
marika.stutzriemer@tu-dresden.de

Subani Gesang
subani_rebecca.gesang@mailbox.tu-dresden.de

Axel Gerdes
gerdes@em.uni-frankfurt.de

Linda Marko
marko@em.uni-frankfurt.de

Cristiano Lana
cristiano.lana@ufop.edu.br

Ulf Linnemann
ulf.linnemann@senckenberg.de

[1] GeoPlasmaLab, Museum Für Mineralogie Und Geologie, Sektion Geochronologie, Senckenberg Naturhistorische Sammlungen Dresden, Königsbrücker Landstraße 159, 01109 Dresden, Germany

[2] TU Dresden, Fakultät Umweltwissenschaften, Institut Für Geographie, Helmholtzstr. 10, 01069 Dresden, Germany

[3] Institut Für Geowissenschaften, Goethe University Frankfurt, Altenhöferallee 1, 60438 Frankfurt am Main, Germany

[4] Frankfurt Isotope and Element Research Center (FIERCE), Goethe-University Frankfurt, Frankfurt am Main, Germany

[5] Programa de Pós-Graduação Em Evolução Crustal E Recursos Naturais, Departamento de Geologia, Escola de Minas, Universidade Federal de Ouro Preto, Morro Do Cruzeiro, Ouro Prêto, MG 35400-000, Brazil

[6] Departamento de Geologia, Escola de Minas, Universidade Federal de Ouro Preto, Morro Do Cruzeiro, Ouro Prêto, MG 35400-000, Brazil

Introduction

The modern sediments of Namibia are an excellent archive to gain knowledge about the mechanisms of sediment transport. This is essential for reconstructing potential routes of sediment movement and provenance, which are frequently used to describe various aspects of palaeogeography and palaeoenvironmental conditions (e.g. Aleinikoff et al. 2008; Gärtner et al. 2017, 2018; Gong et al. 2013; Hofmann et al. 2015; Montes et al. 2015; Moura et al. 2008; Niemi 2013). Aside the geoscientific studies, there is also large interest of studying sediment or dust movement to lower negative effects on aviation (Middleton 2017; Nickovich et al. 2021). Large parts of Namibia are characterised by a hyper-arid to arid climate (Kaseke et al. 2016) that weakens chemical weathering, and thus, results in mainly physical sediment transport processes (Garzanti et al. 2017a). Such extreme conditions typically lead to a very thin and patchy cover of vegetation (Atlas of Namibia Project 2002). Meanwhile, enormous amounts of loose sand form dunes in aeolian transport corridors, which allow distinguishing mean directions of wind (Miller 2008). Additionally, few perennial and many episodic rivers as well as a monodirectional coastal current regime (Garzanti et al. 2017a) largely determine the course of modern sediment transport. These environmental parameters provide outstanding possibilities for studying the entire process that moves sediments from source to temporary sinks, which are subsequently recycled again. They further facilitate detection and observation of potential areas where sediments are mixed and to reveal possible sediment traps that eventually stall material for a long time.

Although remarkable advances in sediment tracking and provenance analysis were accomplished, e.g. by discovering the Orange sand highway (Garzanti et al. 2017a), residence times of sand in the Namib desert (Vermeesch et al. 2010), or the provenance of the northern Kalahari Basin's sediments (Gärtner et al. 2014), still little is known about the complicated network of sediment fluxes. The study, therefore, aims to contribute to the understanding of sediment transport mechanisms in Namibia using a combination of U-Th-Pb-Hf detrital zircon age determination from modern sands all over Namibia, the corresponding zircon grain morphology, and extensive zircon age databases.

Geomorphological and geological setting

Large parts of Namibia and southern Angola are covered by unconsolidated Quaternary sands of mostly unknown origin. Reconstructing their provenance is often done analysing the age spectra of detrital zircon grains. Recently, the number of such studies increased significantly in Namibia and adjacent areas (Gärtner et al. 2014; Garzanti et al. 2014a, b, 2017a, b; Iizuka et al. 2013; Klama 2008; Rino et al. 2008; van der Westhuizen 2012; Vermeesch and Garzanti 2015; Vermeesch et al. 2010). However, most of the studies are restricted to the Orange River system and coastal deposits, while only a minor number of samples were taken from other rivers or dunes (Gärtner et al. 2014; Garzanti et al. 2017b; Vermeesch et al. 2010). Prior to modelling sediment transport as precise as possible, detailed information about the oceanic currents, winds, topography, and river systems, as well as the known zircon age spectra of potential source areas are required.

Known patterns of sedimentary fluxes in southern Africa

The cold Benguela Current is the eastern border of the South Atlantic Gyre (Peterson and Stramma 1991; Wedepohl et al. 2000) and follows the Namibian coast in a north-northwest direction (Fig. 1). This constant current leads to a coast-parallel northward movement of sediments as exemplarily shown by Garzanti et al. (2017b), Ribas et al. (2013), and Ward (1989). The warm, southward flowing Angola Current

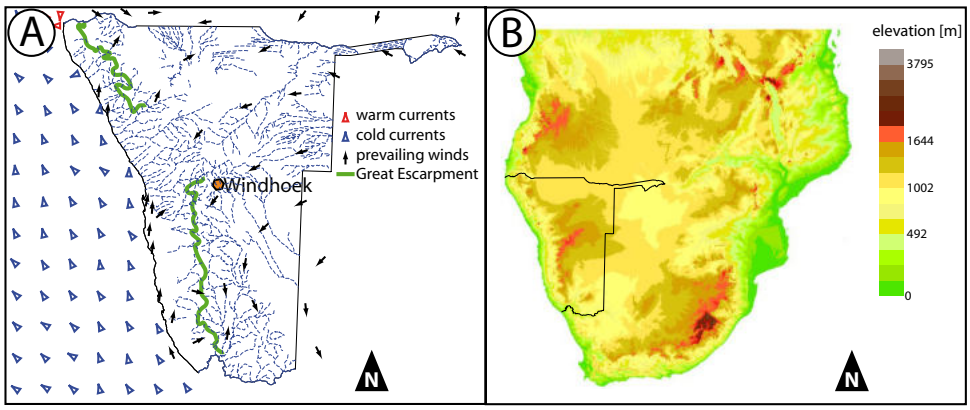

Fig. 1 Prevailing winds and ocean currents of Namibia (left, compiled from Corbett 2018; Gyory et al. 2004; Hipondoka et al. 2014; Shi et al. 2001) as well as relief characteristics (right). A colour version of this figure is available in the online edition of this article

occurs only very close to the coast and converges at approximately 15° S with the Benguela Current (Gyory et al. 2004). It seems that the northward, coast-parallel sediment transport from the Orange River region is suddenly stopped close to this convergence point near the city of Namibe in southern Angola (Garzanti et al. 2017a).

Winds move large amounts of sand in Namibia and are an important driving force for sediment transport. The patterns of predominant wind directions differ throughout the country (Corbett 2018; Lancaster 1982; Mwiya 2015; Shi et al. 2001; Ward 1984), but are mostly stable throughout the year (e.g. Barnes 1999; Mwiya 2015). Winds in the coastal regions are mainly coming from the south to south-southwest, while they blow steadily from north-northeast, east-northeast, or east in the central and eastern parts of Namibia (Crouvi et al. 2010). In the region west of the Great Escarpment, the winds are mostly coming from the west, i.e. from the coast. Prevailing winds from north-northeast are characteristic for the northeastern areas of the country. The Congo Air Boundary to the northwest of the Etosha Pan separates the latter from mainly northwestern winds (Hippondoka et al. 2014). However, exceptions from these patterns occur sporadically, as shown, e.g. by Dansie et al. (2017), where winds from the east transport dust to the offshore regions of Namibia (Fig. 1).

Namibia's drainage is characterised by numerous ephemeral rivers. The only exceptions are the Orange, Kunene, Okavango, Cubango and Zambezi rivers that are perennial and mark the northern and southern borders of the country. The river network of Namibia can be subdivided into the following five main groups: (1) A small number of rivers in Namibia are part of the Kunene River catchment (Nicoll 2010; Strohbach 2008 and references therein). Draining to the northeast, they reach the westward heading Kunene River that discharges into the Atlantic Ocean. (2) The entire central northern regions of Namibia belong to the endorheic Etosha Pan catchment area (Hipondoka et al. 2014; Strohbach 2008). (3) Most rivers northeast of Windhoek flow to the northeast, while those coming from Angola run to the southeast, all terminating in the endorheic Okavango Delta (Gärtner et al. 2014; Strohbach 2008). Exceptions are the Cuando and Zambezi rivers, which reach the Indian Ocean. (4) All rivers west of the Great Escarpment as well as the Ugab and Swakop systems, which have their sources further east, flow to the west or west-southwest until they (sporadically) reach the Atlantic Ocean (Strohbach 2008). (5) The rivers east of the Great Escarpment and south of Windhoek run to the south or southeast until they reach the Orange River that flows west to terminate in the Atlantic Ocean (Strohbach 2008). Palaeoclimate proxies for the past 2000 years seem to indicate relatively humid conditions for the last two centuries (Burrough and Thomas 2013; Nash et al. 2016), which is in line with an increased number of floods in the same time (Greenbaum et al. 2014) and may result in a comparatively high amount of stochastically occurring modern fluvial sediment transport (Gärtner et al. 2020).

General geological setting and zircon age provinces of the Congo and Kalahari cratons

Dated detrital zircon populations found in modern sands are thought to represent the zircon age patterns of their host rocks and, therefore, bear information about their provenance. As detrital zircon data of Namibia's modern sands suggest possible (polycyclic) ultra-long transport from different directions and multiple, partly homogenised sources (Gärtner et al. 2014; Garzanti et al. 2014a; 2017a; Zieger et al. 2020a), a brief summary of the main geologic structures in and around the study area as well as beyond the current catchment boundaries of the Namibian drainage system is required (Fig. 2). Detailed information about timing of orogenic processes, tectonic settings, lithologies, stratigraphy, etc. can be found in the literature, given in the online resources (Table S4), and references therein. Such a transcratonal view is necessary, as past studies showed severe and large-scaled changes in drainage directions and source areas (Gärtner et al. 2014; Houben et al. 2020; Moore et al. 2007) or suggest switching river courses over time (Bluck et al. 2007), leading to sediment sources of unexpected provenance that could now be reworked by the Namibian rivers. Equally rapid reorganisations of drainage systems in a continental scale were also reported from several places throughout Earth's history (Blum and Pecha 2014; Caputo and Soares 2016; Zhang et al. 2019).

The composite Kalahari and Congo cratons represent the two main entities in the study area. Both of them expose a complex geologic history including numerous orogenic belts and terranes along their margins (Begg et al. 2009; De Waele et al. 2009; Jacobs et al. 2008; McCourt et al. 2013; Zeh et al. 2009). Archaean nuclei of both cratons are the Tanzania (Kabete et al. 2012), Zimbabwe (Jelsma et al. 1996) and Kaapvaal (Wilson and Zeh 2018) cratons, of which the latter covers large areas of the upper Orange River catchment. The West Nile (Thiéblemont et al. 2018), Northeast Congo (Siegesmund et al. 2018) and North Uganda blocks (Saalmann et al. 2016), but also the Dodoma System (Thomas et al. 2016) and the Limpopo Belt (Kröner et al. 2018) are located in the eastern parts of the Congo and Kalahari cratons. Further Archaean components are the Kasai Block (Walraven and Rumvegeri 1993) in the south-central Congo Craton, the Ntem Chaillu Block (Tchameni et al. 2010) and the oldest parts of the Angola Shield (De Carvalho et al. 2000; Gärtner et al. 2016) in its northwestern and western realm (e.g. Begg et al. 2009; Thiéblemont et al. 2018; Fig. 2). Particularly, the Angola Shield is thought to

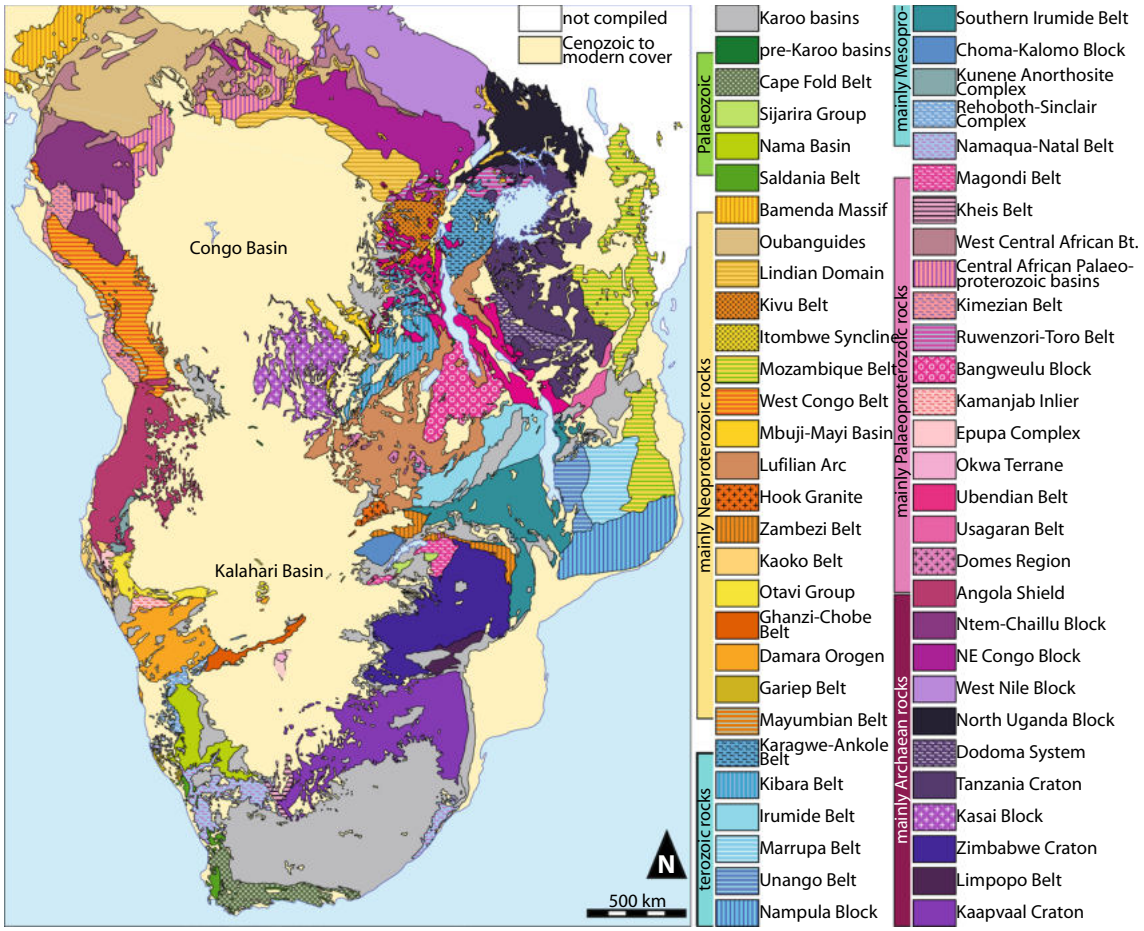

Fig. 2 Simplified geological map of southern Africa showing the approximate location and extent of the main tectonic units (compiled from Begg et al. 2009; Frimmel et al. 2006; McCourt et al. 2013; Siegesmund et al. 2018; Tack et al. 2001; Westerhof et al. 2014; and references therein). A colour version of this figure is available in the online edition of this article

contribute a significant amount of siliciclastic detritus to the northern Namibian rivers (Gärtner et al. 2014).

Palaeoproterozoic igneous units and orogenic belts are abundant in southern Africa and can be found all around and within the Kalahari and Congo cratons (Fig. 2). With respect to the modern Namibian drainage system, the most important features of Palaeoproterozoic age are the Angola Shield (Jelsma et al. 2018), the Epupa Complex (Kröner et al. 2015) and the Kamanjab Inlier (Kleinhanns et al. 2015) that are drained by the northern and central Namibian rivers, as well as the Kheis Belt (van Niekerk 2006), which is part of the Orange River catchment. Palaeoproterozoic structures like the Bangweulu Block (De Waele and Fitzsimmons 2007) or the Ubendian Belt (Ganbat et al. 2021) are currently not drained by any of the Namibian Rivers.

The occurrence of Mesoproterozoic orogens is limited to the northern and northwestern parts of the Kalahari Craton–Namaqua-Natal Belt (Eglington and Armstrong 2003), Rehoboth-Sinclair Complex (van Schijndel et al. 2014), both of them within the Namibian drainage system—as well as the entire eastern margin of both cratons (Karagwe-Ankole Belt, Kibara Belt, Irumide Belt, Southern Irumide Belt, Choma-Kalomo Block; De Waele et al. 2009; Fernandez-Alonso et al. 2012; Glynn et al. 2017; Hauzenberger et al. 2014; Kokonyangi et al. 2007; Villeneuve et al. 2019; Fig. 2). An exception is the Kunene Anorthosite Complex in northern Namibia and southern Angola (e.g. Drüppel et al. 2007), drained by the Kunene River and its tributaries.

The collision of the Kalahari and Congo Cratons with several other terranes and cratons during the Neoproterozoic–Early Cambrian assembly of Gondwana led to the formation of several orogenic belts, which are simplistically summarised as pan-African orogens (e.g. Goscombe et al. 2018; Oriolo and Becker 2018). Accordingly, rocks of this age occur around the entire Congo Craton and can be found on the southern, western and northern margins of the Kalahari Craton as well (Fig. 2). Among this large group of orogenic belts there are the Gariep (Hofmann et al. 2013), Kaoko (Konopásek et al. 2017) and Damara belts (Nieminski et al. 2019), which are currently drained by the Namibian

river network. Remarkably, the Orange River as one of the largest streams in Africa does not drain significant areas of pan-African age until its mouth to the Atlantic (Iizuka et al. 2013; Fig. 2), which is due to the long-lived stability of the Kaapvaal Craton (Pearson et al. 2021).

Vast areas of southern Africa are covered by Carboniferous–Permian to Triassic Karoo-type sediments (Catuneanu et al. 2005; Linol et al. 2015; Zieger et al. 2019, 2020a, b) or younger strata (Haddon and McCarthy 2005; Ringrose et al. 2008; Vermeesch et al. 2010). Numerous dykes, as well as plutonic and volcanic rocks of Jurassic to Cretaceous age, occur along the western coast of southern Africa (Comin-Chiaramonti et al. 2011; Hastie et al. 2014). They are interpreted as result of the Atlantic Ocean opening (Comin-Chiaramonti et al. 2011). The youngest igneous activities within the study area are the ca. 37 Ma old mafic intrusions along the Atlantic coast of the Namibian Sperrgebiet area, e.g. Klinghardt phonolite (Kröner 1973), or the ca. 32 to 35 Ma Aris phonolite south of Windhoek (Burger and Walraven 1976; Fitch and Miller 1984). Due to their paucity in zircon, these youngest igneous rocks likely do not contribute any detectable signal to the detrital zircon record.

Methods

Sample preparation

Heavy mineral separation was achieved from the < 400 µm fraction of the sands using lithium heteropolytungstate in water prior to magnetic separation in the Frantz isomagnetic separator. Final selection of representative zircon for U–Pb dating (Fedo et al. 2003; Link et al. 2005) was carried out by randomly hand-picking about 150 grains of all sizes, colours and shapes under a binocular microscope (ZEISS Stemi 2000-C). Subsequently, morphotypes (Pupin 1980), length and width, roundness and surface structure (Gärtner et al. 2013) were determined using a scanning electron microscope (SEM, ZEISS EVO 50). These morphological characteristics supplement the isotopic data and may help to improve the precision of provenance studies. Finally, zircon grains were mounted in resin blocks and polished to half their thickness to expose their internal structure. Cathodoluminescence (CL)-imaging was performed using the SEM coupled to a HONOLD CL-detector operating at 550 nm spot size and 20 kV.

U-Th-Pb age determination via LA-ICP-MS

Zircon areas showing monophase growth patterns were preferentially selected for isotope analyses in order to avoid mixed U–Pb ages resulting from different late- to post-magmatic or metamorphic influences. Measurements for U, Th and Pb were conducted at the GeoPlasma Lab, Senckenberg Naturhistorische Sammlungen Dresden using Laser Ablation with Inductively Coupled Plasma Mass Spectrometry (LA-ICP-MS) techniques. A Thermo-Scientific Element 2 XR instrument coupled to an ASI RESOlution SE S155 193 nm Excimer Laser system was utilised. Ablation happened in a Laurin Technic S155 ablation cell, which enables sequential sampling of heterogeneous grains (e.g. growth zones) during time-resolved data acquisition. Single spot measurement contained 15 s background acquisition followed by 30 s data acquisition and 15 s washout. The spot sizes ranged between 25 and 35 µm. Detailed specifications on the instrument settings are available in online resource (Table S1). Common-Pb correction, based on the interference- and background-corrected ^{204}Pb signal and a model Pb composition (Stacey and Kramers 1975), was carried out if necessary. Judgement of necessity for correction depended on whether the corrected ^{207}Pb/^{206}Pb lay outside the internal errors of the measured ratios. A U–Pb analysis is concordant when it overlaps with the Concordia within uncertainty. So, it seems to be appropriate to exclude results with a low level of concordance (^{206}Pb/^{238}U age/^{207}Pb/^{206}Pb age × 100), but very large errors that overlap with the Concordia from interpretation. An interpretation with respect to the obtained ages was done for all grains within the commonly used concordance interval of 90–110% (^{206}Pb/^{238}U age/^{207}Pb/^{206}Pb age × 100, e.g. Spencer et al. 2016). Discordant analyses were generally interpreted with caution, i. e. they were discarded in this study. Raw data were corrected for background signal, common-Pb, laser-induced elemental fractionation, instrumental mass discrimination, depth- and time-dependant elemental fractionation of Pb/Th and Pb/U by use of an Excel® spreadsheet program developed by Axel Gerdes (Institute of Geosciences, Johann Wolfgang Goethe-University Frankfurt, Frankfurt/Main, Germany). Measurement of Th-U ratios was carried out parallel to U-Th-Pb determination with the same combination of instruments. Reported uncertainties were propagated by quadratic addition of the external reproducibility obtained from reference zircon GJ-1 (~ 0.6% and 0.5–1.0% for the ^{207}Pb/^{206}Pb and ^{206}Pb/^{238}U, respectively, Jackson et al. 2004) during individual analytical sessions and the within-run precision of each analysis. Plesovice reference zircon was used as secondary standard and yielded results in the published range (Sláma et al. 2008). For zircon grains older than 1 Ga, ^{207}Pb/^{206}Pb ages were taken for interpretation, while ^{206}Pb/^{238}U ages were used for younger grains. For further details on analytical protocol and data processing see Gerdes and Zeh (2006). Kernel density estimate (KDE) plots were produced using the *detzrcr* package (Andersen et al. 2018a). Non-metric multi-dimensional scaling (MDS) plots are based on the Kolmogorov–Smirnov statistical analysis (Vermeesch 2013) and were made with the *provenance* package of Vermeesch et al. (2016). Both of the

latter packages were designed for the open source statistical program R, of which version 4.0.5 was applied.

Hf-isotopes

Hafnium isotope analyses were preferentially done on areas overlapping with concordant U–Pb spots. The procedure followed the method described in Gerdes and Zeh (2006; 2009). Measurements were realised via Thermo-Finnigan NEPTUNE multi collector ICP-MS at Universidade Federal de Ouro Preto coupled to a RESOlution M50 193 nm ArF Excimer (Resonetics) laser system. Spot sizes ranged from 26 to 40 µm in diameter, while ablation was carried out with a repetition rate of 4.5–5.5 Hz and an energy density of 6 J/cm^2 during 50 s of data acquisition. Correction of the instrumental mass bias for Hf isotopes was done using an exponential law and a $^{179}Hf/^{177}Hf$ value of 0.7325. The mass bias for Yb isotopes was corrected using the Hf mass bias of the individual integration step multiplied by a daily βHf/βYb offset factor (Gerdes and Zeh 2009). All data were calibrated relative to the JMC475 of $^{176}Hf/^{177}Hf$ ratio = 0.282160, while quoted uncertainties are quadratic additions of the within run precision of each analysis and the reproducibility of the JMC475 (2 SD = 0.0028%, $n = 8$). Accuracy and external reproducibility of the method was verified by repeated analyses of GJ-1, 91,500 and Temora reference zircons, which yielded a $^{176}Hf/^{177}Hf$ of 0.282018 ± 0.000076 (2 SD, $n = 47$), 0.282297 ± 0.000038 (2 SD, $n = 21$) and 0.282610 ± 0.000416 (2 SD, $n = 20$), respectively. This is in agreement with previously published results (e.g. Gerdes and Zeh 2006; Sláma et al. 2008) and with the LA-MC-ICPMS long-term average of GJ-1 (0.282010 ± 0.000025; $n > 800$) reference zircon at Frankfurt Isotope and Element Research Centre (FIERCE), Johann-Wolfgang-Goethe University Frankfurt (Frankfurt/Main). Initial $^{176}Hf/^{177}Hf$ values are expressed as $\varepsilon Hf_{(t)}$ calculated using a decay constant value of 1.867 10^{-11} year^{-1} (Scherer et al. 2001), CHUR values according to Bouvier et al. (2008; $^{176}Hf/^{177}Hf_{CHUR,today} = 0.282785$ and $^{176}Lu/^{177}Hf_{CHUR,today} = 0.0336$) and the apparent zircon ages were obtained for the respective domains. The calculation of Hf two-stage model ages (T_{DM}, expressed in Ga) was performed using the measured $^{176}Lu/^{177}Lu$ of each spot, a value of 0.0113 for the average continental crust and ratios for juvenile crust of $^{176}Lu/^{177}Lu_{NC} = 0.0384$ and $^{176}Hf/^{177}Hf_{NC} = 0.283165$ (average MORB; Chauvel et al. 2008).

Results

In total, 4771 zircon grains were extracted from 30 samples. Each grain was analysed for its length, width, morphology (Gärtner et al. 2013) and morphotype (Pupin 1980). To obtain a more complete picture of detrital zircon morphology of modern Namibian sands, data from northern Namibian rivers (Gärtner et al. 2014) were included in the morphological analyses. U–Pb ages and Th–U isotope compositions were analysed at 4679 zircon grains (4698 spots) of the same 30 samples. In total, 2910 of 4698 U–Pb analyses yielded ages within the concordance interval between 90 and 110%. Only the latter data were used for interpretative purposes. Additionally, samples NAM-O-8, NAM-O-18, NAMA014 and NAMA023, as well as samples NAM-O-23 and NAM-O-30 published by Gärtner et al. (2014) were analysed for their Hf-isotope composition. Due to the large amount of samples and data, the results are presented in a summarised manner, whereas the complete data for each individual grain is given in the online resources (Tables S2 and S3).

Concerning their morphology, zircon grains from aeolian sediments show a much narrower range in grain size distribution (Fig. 3a) and a larger mean grain size—length 163 µm, width 79 µm—than those from fluvial deposits—length 134 µm, width 66 µm. Particularly the depletion of aeolian zircon populations in sediments finer than about 80 µm has a striking difference to fluvial transported zircon (Fig. 3b). Furthermore, almost all mean size values of aeolian zircon grain samples overlap with each other within standard deviation (Fig. 3c), which is not the case for zircon grain populations deposited in fluvial systems (Fig. 3d). There is almost no difference in width–length ratios between aeolian (0.51) and fluvial (0.52) zircon populations. Although the mean roundness in both zircon groups is very similar at 6.69 and 6.47 (Fig. 4), differences in the distribution of roundness are expressed by the presence of secondary maxima between 7 and 8 in most of the aeolian zircon populations. Such distribution patterns are subordinate in fluvial sediments. Mean surficial pitting of the detrital zircon grains ranges from 1.46 to 2.42. There is almost no difference between zircon from dune (mean 1.94) and river sands (1.89), while beach sample NAMA051 shows a slightly higher number (2.12). Finally, the morphotype distributions show more or less similar patterns throughout southern Namibia, while morphotype variety is highest towards the north (Fig. S1). Particularly the detrital zircon populations in southern and central Namibia are characterised by high amounts of morphotypes assigned to high temperatures (mostly S23, S24, S25). Remarkably, the proportions of zircon morphotypes indicating lower temperatures during formation increase towards the north.

Hereafter, zircon ages of the analysed samples are summarised for regions with similar age-distribution patterns.

SW Namibia

Starting in the SW parts of Namibia, which are dominated by the Orange River, its tributaries and the southern Namib Sand Sea, the general zircon age distribution pattern is

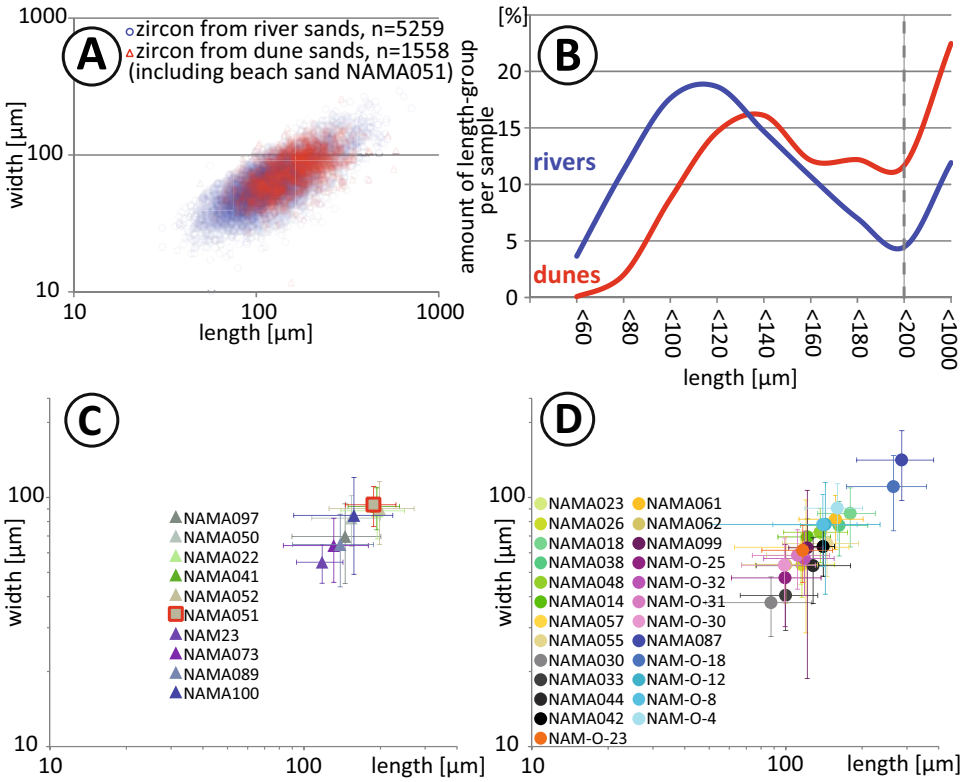

Fig. 3 Summary of some morphological characteristics of the studied samples and those of Gärtner et al. (2014); **a** length and width of zircon from river and dune samples; **b** length distribution of zircon from river and dune samples; **c** average length and width of detrital zircon from dune and beach samples; **d** average length and width of detrital zircon from river samples; crosses in **c** and **d** indicate the standard deviation. A colour version of this figure is available in the online edition of this article

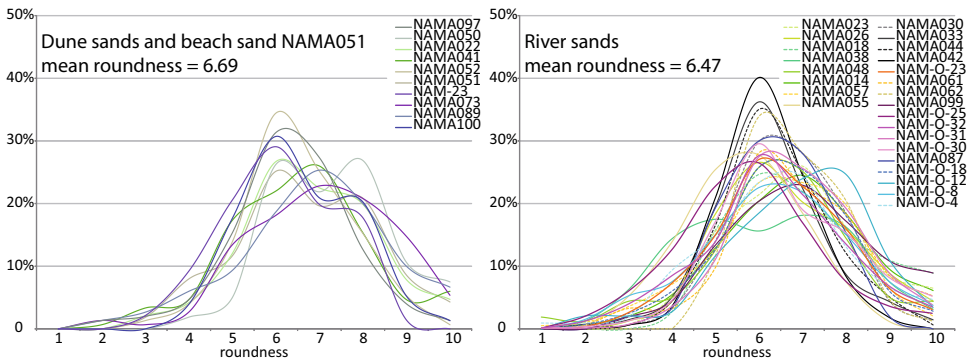

Fig. 4 Distribution of the roundness according to Gärtner et al. (2013) for samples of dune and beach sands (left) and samples taken from rivers (right). A colour version of this figure is available in the online edition of this article

largely characterised by mid to late Mesoproterozoic, mid to late Neoproterozoic and early Cambrian main populations. Minor peaks are formed by Palaeoproterozoic, mostly Orosirian ages, but are scarce in dune sands. Few zircon grains yielded Permian and late Carboniferous ages, while Triassic or even Jurassic detritus is limited to few single grains (Fig. 5). Sample NAM-O-8 from the middle reaches of the Fish River is different from most other samples in SW Namibia as it contains many Palaeoproterozoic but only few Ediacaran-Cambrian zircon grains. A slightly elevated Palaeoproterozoic age peak is also present in samples NAM-O-12 and NAM-O-18, of which the last sample was taken only some km downstream the mouth of the Fish River.

SW-central Namibia

Going to the SW-central Namibian realm, which is approximately the region between the Swakop River, the Great Escarpment and the Kaukausib River south of Lüderitz, the detrital zircon age patterns of samples from the Namib Sand Sea and the coastal regions apparently mirror those from the Orange River. Nevertheless, the detritus of smaller catchments sometimes has completely different main peaks, as exemplarily shown for sample NAMA038 (no. 7 in Fig. 5), where the sediments of the Gaub River are mostly composed of Palaeoproterozoic and Mesoproterozoic grains, while any younger ages are scarce. Furthermore, it has to be highlighted that samples taken in close vicinity to the coast are

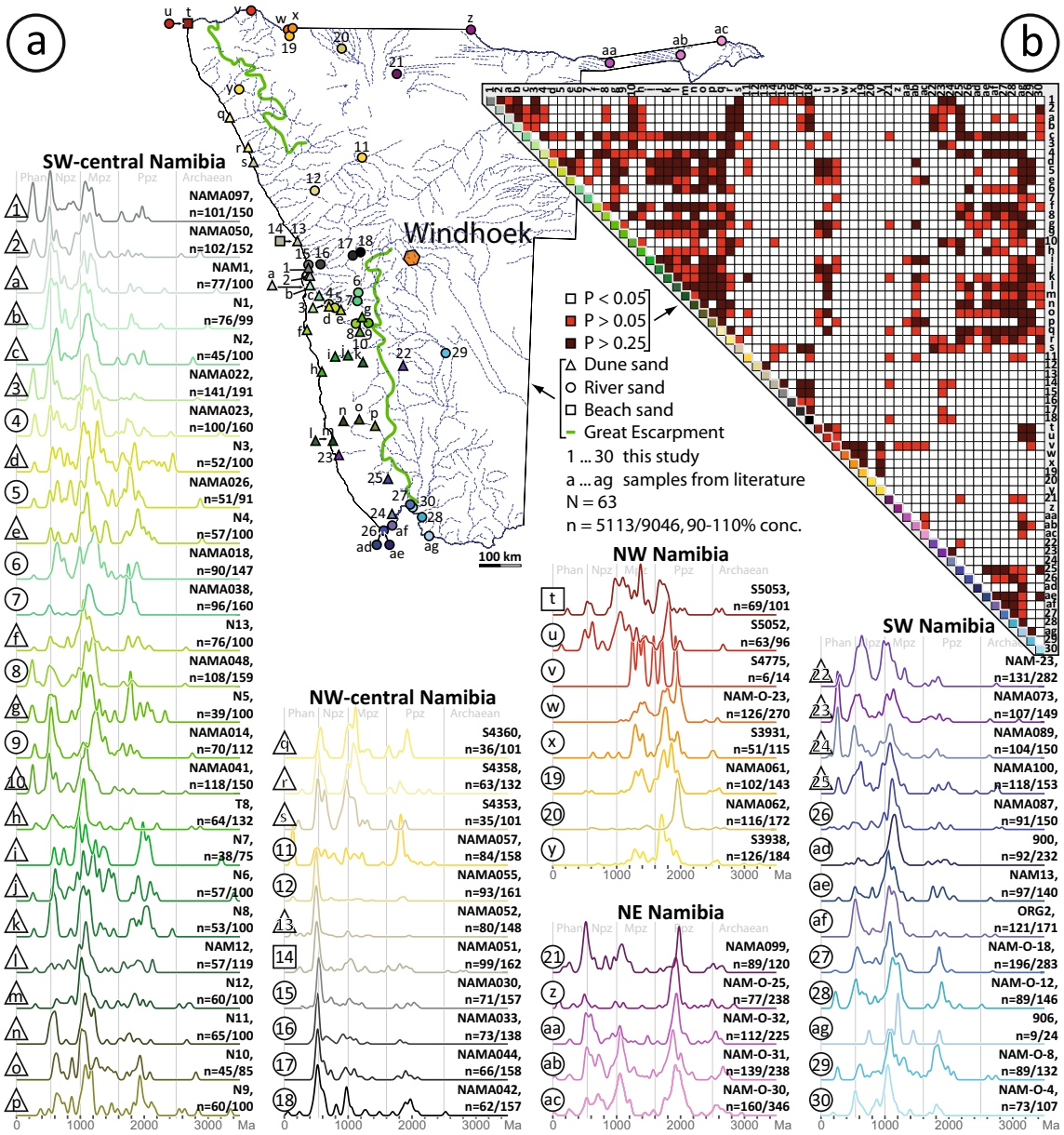

Fig. 5 Kernel Density Estimates (KDE) of detrital zircon from modern sands (Gärtner et al. 2014; Garzanti et al. 2014a; 2017a; Iizuka et al. 2013; Klama 2008; Vermeesch et al. 2010; and this study). A colour version of this figure is available in the online edition of this article

significantly depleted in Palaeoproterozoic zircon compared to those samples near the Great Escarpment.

NW-central Namibia

Detrital zircon age patterns of sands in NW-central Namibia—which is roughly the area between the Swakop River, the Great Escarpment including the catchment areas of larger ephemeral rivers such as Swakop and Ugab and the Hoanib River—are fundamentally different to those from the south. Here, a late Neoproterozoic–Cambrian peak often represents more than 50 and sometimes up to ~ 80% of the detrital zircon ages within one sample (Fig. 5). Furthermore, sediments from the Swakop catchment often lack any post-Cambrian zircon, while smaller populations of various Permo-Carboniferous to Early Cretaceous age occur further north. A special case is represented by modern Ugab sample NAMA057, which has a main peak formed by Palaeoproterozoic zircon, comparatively small amounts of Meso- and Neoproterozoic ages, but remarkable portions of Mesozoic grains (Fig. 5).

NW Namibia

Northwestern Namibia is almost entirely drained by the Kunene River, whose sands are characterised by Palaeoproterozoic to late early Mesoproterozoic detrital zircon, which seems to be a unique marker population throughout Namibia. Consequently, any younger or older zircon grains are limited to single grains. Remarkably, sample NAMA062 from the Etaka River in the Oshana system of the Cuvelai-Etosha Basin is characterised by almost entirely Orosirian zircon grains.

NE Namibia

Finally, the northeastern Namibian sediments between the Cubango Megafan in the west and the Zambezi River in the east contain large amounts of mid Palaeoproterozoic and late Mesoproterozic detrital zircon, while the frequency of late Neoproterozoic to early Palaeozoic zircon decreases from west to east. Sediments sampled in this region host less frequent but regularly occurring zircon populations of late Neoarchaean age. Remarkably persistent occurrences of Permo-Carboniferous zircon are even less abundant. All post-Palaeozoic ages are scarce but can be as young as the Neogene–Palaeogene transition at ca. 23 Ma.

The Hf isotope record obtained from sands of modern Namibian rivers is quite similar throughout the country (Fig. 6). Most of the zircon grains have $\varepsilon Hf_{(t)}$ values between ca. -15 and 10, with more than half of them showing positive values. Large spreads in $\varepsilon Hf_{(t)}$ values were found in all major zircon age populations with largest variations in mid to late Neoproterozoic-Cambrian times (pan-African orogeny s. l.). There is only one characteristic that allows distinguishing the two groups from each other: the amount of detrital zircon indicating formation from mostly Neo- and Mesoarchaean crust. Such grains seem to occur more frequently in perennial rivers (Kunene, Zambezi, Orange) that drain Archaean basement, while they are very rare in ephemeral rivers that originate in the central Namibian highlands.

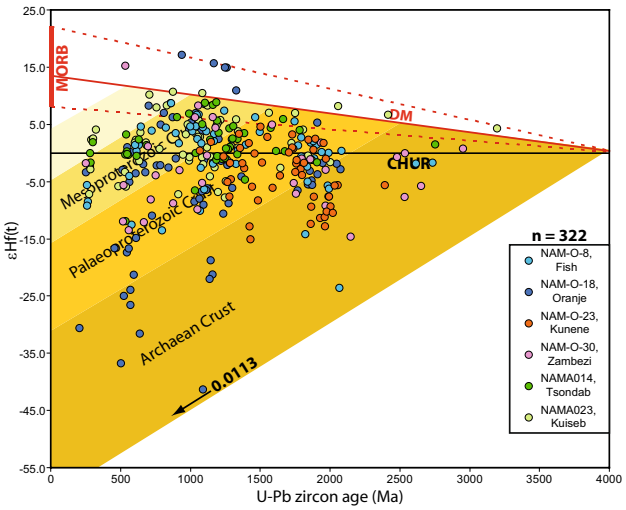

Fig. 6 Diagram of $\varepsilon Hf_{(t)}$ values versus concordant U–Pb zircon age for six samples of the present study. Note the wide spread of values for most samples indicating potential crustal mixing. $\varepsilon Hf_{(t)}$ data were calculated using the decay constant of 1.867 10^{-11} $year^{-1}$ (Scherer et al. 2001) and the CHUR parameters of Bouvier et al. (2008). Further details and references of depleted mantle evolution are given in Gerdes and Zeh (2006; 2009) and Dhuime et al. (2011). A colour version of this figure is available in the online edition of this article

Discussion

Remarks on zircon morphology

Detrital zircon grain morphology still is an underrated tool when analysing sediment provenance and thus, such parameters often remain unlogged. However, the number of combined isotopic and morphological studies currently seems to increase (e. g. Augustson et al. 2018; Bónová et al. 2020; Osorio-Granada et al. 2020). These data from different environments allow drawing first assumptions on the transport processes including transport media and the amount of multiply-recycled vs. first (or low number) cycle material.

The data from this study show—at least for the Namibian case—that average grain sizes vary a lot in fluvial deposits, while the range is quite narrow in aeolian sediments (Fig. 3). Not only are the average grain sizes of fluvial and aeolian samples very different, but also the overall range of grain sizes in both groups differs significantly. Thus, the smallest grains detected in fluvial samples have lengths of about 30 µm, while the smallest grains of dune sands are rarely shorter than 60 µm. Similar phenomena were reported from other arid regions like the Taklimakan Desert (Jiang and Yang, 2019). Given the different settling velocities for zircon grains of variable sizes, shapes and roundness in fluvial and aeolian transport regimes (Cantine et al. 2020; Garzanti et al. 2008; and references therein) it is possible to estimate the lower and upper boundaries of the energy that is needed to keep the grains in motion/suspension or to deposit them. With respect to the aeolian sediments it can be assumed that (in average) the steady winds have enough energy to transport almost all zircon grains < 60 µm out of the sampled areas, to move most of the grains between 60 and ca. 200 µm, but do normally not transport larger grains over longer distances (Fig. 3). Accordingly, the energy to keep the sub-60 µm grains moving must at least equal the settling velocity of a 60-µm zircon in air (Cantine et al. 2020; Garzanti et al. 2008). A special, selective effect for such

small particles may be related to the quasi-periodic structure of dunes and their alignment to the main wind direction. Dune formation is dominated by the transport properties of quartz and this influences the average transport velocity of zircon particles differently from that of quartz, due to the density difference of the two materials (Cantine et al. 2020; Garzanti et al. 2008). Particles have a vertical downward force proportional to the 3rd power of the diameter, while friction is proportional to surface (2nd power) of the diameter and total speed, which may be dominated by the wind speed for small particles. This means a big difference for the free flight of large and small particles starting at the top with an upward direction defined by the dune's angle close to and before its top. Given that particles with a diameter below a critical value are able to reach the area close to the next dune top, than larger particles fall down earlier due to their higher mass. Accordingly, the latter then have to move larger distances in low wind speed corridors along the bottom part of the dune slope. This difference in transport speed is amplified by the quasi-periodic dune structure of the dunes when repeating this process. Thus, the probability to find a particle of a given diameter is proportional to its travel time and secondary effects of dune movement. Hence, the presence of fast moving (small) particles in a dune is a dramatically decreased by increasing transport distance. For different materials the density and friction-influencing shape parameters may be the most discriminating factors in the diameter distribution. Currently, this purely hypothetical statement is based on the obtained data. However, this grain size-dependant bias is seemingly not studied in detail for zircon and the assumed effect on transport is purely qualitative. Further bias may be introduced by sample altitudes, as aeolian sediments are characterised by decreasing grain sizes with increasing altitude (Goosmann et al. 2018). Finally, sediments in fluvial and coastal environments are prone to hindered settling of sand–mud suspensions due to the proximity of other sediment particles in high-density clouds (Shakeel et al. 2020; Spearman and Manning 2017). Such effects are not yet described for aeolian sediments (excluding ash-falls). These kinds of grain size sorting induce a natural bias between fluvial and aeolian samples, which might have to be taken into account when reconstructing provenances.

Furthermore, fluvial transport itself introduces bias to the detrital zircon record, as, e.g. metamict grains disappear early in the transport process (Markwitz et al. 2017). Although it seems plausible that older zircon is much more likely to be transported for longer distances in multiple cycles of erosion and sedimentation than younger zircon and, therefore, tends to be smaller in average (Augustson et al. 2018; Lawrence et al. 2011; Markwitz et al. 2017), there are some regions that do not show this trend at all (e.g. Gärtner et al. 2014; Muhlbauer et al. 2017) or even reveal a reverse correlation (Gärtner 2017). The latter observations illustrate the necessity for intensified studies on zircon grain morphology and its correlation to other parameters like age, basement exposure, etc.

Roundness (Fig. 4), but also the width/length ratio (Fig. 3) of detrital zircon can be used as a parameter of already achieved transport distance (Gärtner et al. 2013; Markwitz et al. 2017; and references therein). Thus, euhedral, less rounded and/or very elongate zircon indicates first cycle sedimentation, while well-rounded and shortened grains are multiply recycled and were transported over longer distances (Gärtner et al. 2017; Leary et al. 2020; Zoleikhaei et al. 2016). This becomes obvious when analysing all concordant zircon grains from modern sands of Namibia with logged roundness (Gärtner et al. 2014; this study, Fig. 7). There, older grains trend to have a higher roundness than younger grains indicating their longer involvement in sediment recycling processes. However, local effects, like samples taken adjacent to outcrops of unaltered igneous rocks, may lead to other roundness distribution patterns for specific samples or even whole areas. Furthermore, the obtained roundness data show that the average roundness is very similar between detrital zircon from river and dune sands (Fig. 4), indicating that at least the last mode of transport does not have a significant impact concerning this feature. A number of six samples (NAMA022; NAMA038, NAMA050, NAMA051, NAMA100, NAM-23) show a roundness distribution pattern with two peaks. Such patterns were previously interpreted to represent input of material from (originally) two different sources, of which one was less often recycled than the other (Gärtner et al. 2018). Remarkably, all of these samples are either in close vicinity to the Great Escarpment of southern and central Namibia, or are downstream the mouth of the Gaub into the Kuiseb River to the coast (Fig. 4). A possible

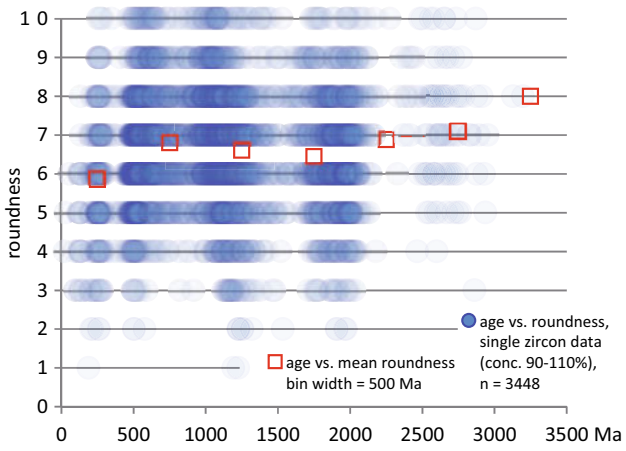

Fig. 7 Age and roundness of the studied zircon grains indicate decreasing roundness with younger ages (for average values of 500 Ma bins). A colour version of this figure is available in the online edition of this article

explanation could be the combination of (meta-) igneous rocks cropping out immediately west of sedimentary successions that are exposed along the Great Escarpment of southern Namibia (e.g. Geological Survey of Namibia 1977; 2000) on the one hand as well as the multitude of different rocks that are present in the Gaub valley on the other (e.g. Geological Survey of Namibia 1994). At least an origin of central Namibian beach and dune sands (e.g. NAMA051, NAMA052) from pure Orange River sediment can be ruled out, as neither the Orange River samples nor the very close dune sample NAMA089 show comparable double-peaked patterns of roundness distribution (Fig. 4).

The surficial pitting of zircon due to transport processes is well known, but rarely cited in the literature (e.g. Rainbird et al. 2001; Stevens et al. 2010), often neither detail about the quantity nor about the morphology of these features are given. Similar to quartz grains (Krinsley and Doornkamp 2011), detrital zircon grains show a broad variance of surficial collision marks and pitting. Due to the different structure of zircon and quartz, it is highly likely that impacts on the one mineral cause other patterns of collision marks than on the other. Furthermore, they may be characteristic for certain transport media and transport energies (Cross and Crispe 2007; Gärtner et al. 2013). Zircon often shows oscillatory zoning, i.e. a lamination of U-rich and U-depleted zones (Nasdala et al. 2003), which likely results in different bonding forces between these zones due to microfractures and leaching (Wayne and Sinha 1988). Thus, zircon grains can show apparently fresh surfaces after collisions or other physical treatment that caused delamination and are often indicated by surficial cracks (Gärtner et al. 2013; Kempe et al. 2004). As the entire process is not fully understood yet, this study is limited to log the quantities of such features, while the individual morphologies will be reported elsewhere. In general, there are no differences concerning the average amount of surficial collision marks when comparing all aeolian and fluvial samples (1.94 vs. 1.89). However, the amount of heavily pitted grains per sample (class 4 according to Gärtner et al. 2013) shows a clear geographic distribution in southern and central Namibia, whereas such grains are less abundant in northern Namibia. Grains with intensely pitted and scratched surfaces were interpreted to possibly originate from (peri-)glacial deposits (Gärtner 2011; Gärtner et al. 2017; Linnemann et al. 2017). Initial studies suggest that even in glacial diamictite or eroded moraine material the amount of such grains rarely exceeds 5% (Gärtner 2011; Zieger et al. 2019). Indeed, most of the samples having an increased amount of heavily pitted zircon grains were sampled in comparatively short distances downstream of glacial deposits or in the prevailing direction of wind from these rocks in southern and central Namibia (Fig. S2). Particularly the lower reaches of the Orange River host multiple outcrops of glacigenic diamictites (Fig. S2), whose detrital zircon grains can widely be distributed. Although glacigenic deposits are also abundant in the northern parts of the country, they mostly consist of calcareous or dolomitic material (Hoffman 2011) and thus, are less fertile in detrital zircon grains. This could be an explanation for the low numbers of corresponding zircon grains in samples from northern Namibia.

The zircon morphotype (Pupin 1980) distribution of detrital zircon grains is a further characteristic that may help to distinguish between samples with similar age patterns. Although increasing length of transport lowers the numbers of distinguishable grains, this process likely does not have an effect on the general morphotype distribution patterns. There have only been few studies that used this features for detrital settings (e.g. Dunkl and Demény 1997; Naing et al. 2014; Osorio-Granada et al. 2017). In the case of Namibian modern sands there is a narrow array of zircon morphotypes in the south with highest amounts for the S24 (Fig. S1) and surrounding morphotypes. This pattern seems to characterise most of the detrital zircon in the Orange and Fish River catchments at least to the area of Mariental in the north (Fig. S1). The spectrum gets wider and more diverse for almost all samples north of the Tsondab River, where zircon grains with S1 to S15 morphotypes (Fig. S1) are more abundant than in the south. This changed pattern has its strongest expression in samples from those rivers that drain the Damara Orogen, but has also been observed for a sample from the Gariep Belt (Fig. S1), as well as for the Kunene, Okavango and Zambezi catchments (Gärtner et al. 2014). Furthermore, this pattern was also observed in dune and beach sands adjacent to the aforementioned regions. Although delamination due to physical treatment can cause fresh surfaces in detrital zircon (Gärtner et al. 2013; Kempe et al. 2004), there are only few cases of differing morphotypes between the outer and the inner parts of one zircon grain (Köksal et al. 2008). Thus, it has to be assumed that zircon morphotype does not change during sedimentary transport. Therefore, it seems appropriate to assume a certain input of detrital zircon from the Damara Orogen and likely also from the Gariep and Kaoko belts for large parts of those areas termed northwest-central and northern southwest-central Namibia (Fig. 5). Additional sources further north may contribute to the sediments of northwest and northeast Namibia (Gärtner et al. 2014). Nevertheless, there are some samples that suggest regional exceptions from this trend, e.g. NAMA038 from the Gaub River, NAMA061 from an unnamed tributary of the Oiva River in the East Kaoko Zone, or NAMA062 from the Etaka River of the Oshana System. The morphotype distribution of these samples resembles those of the Orange-Fish River drainage system further south. Proving a possible correlation of zircon morphotype distribution and less recycled orogenic material as possibly indicated by the data requires more

research. Nonetheless, input of non-Orange River detrital zircon to the coastal regions of central Namibia cannot be neglected.

Detrital zircon age patterns and Hf-isotopes

The evaluation of the available zircon age data including the results of this study begins in the south at the Orange River and ends in the north at the Kunene River, thus following the Orange sand highway as proposed by Garzanti et al. (2017a). However, this study also aims to analyse processes of sediment transport in the less-studied Namibian hinterland. All information provided by the obtained detrital zircon age distribution patterns is supplemented by a zircon age and Hf-isotope data base for the Kalahari and Congo cratons exceeding 100,000 single zircon age analyses of more than 2370 samples (Fig. 8; Tab.S4). Concerning the assumed high degree of sediment recycling and homogenisation through time (e.g. Zieger et al. 2020a; b), such a data base is prerequisite when aiming to reconstruct potential tracks of sediment transport.

The detrital zircon age patterns of the lowermost parts of the Orange River are characterised by a Tonian-Stenian (ca. 950–1100 Ma) main peak. Rocks of comparable age are abundant in the Namaqua Belt (Bailie et al. 2012; Macey et al. 2018) that is drained by the river. An Orosirian subpeak (~2000 Ma) is also present in all Orange River samples of this and of earlier studies (e.g. Iizuka et al. 2013; Klama 2008; Vermeesch et al. 2010). What remains enigmatic is the Cambrian–Ediacaran (~520–600 Ma) peak that occurs in many samples of the lower Orange River (Iizuka et al. 2013; Vermeesch et al. 2010; this study; Fig. 5). There are

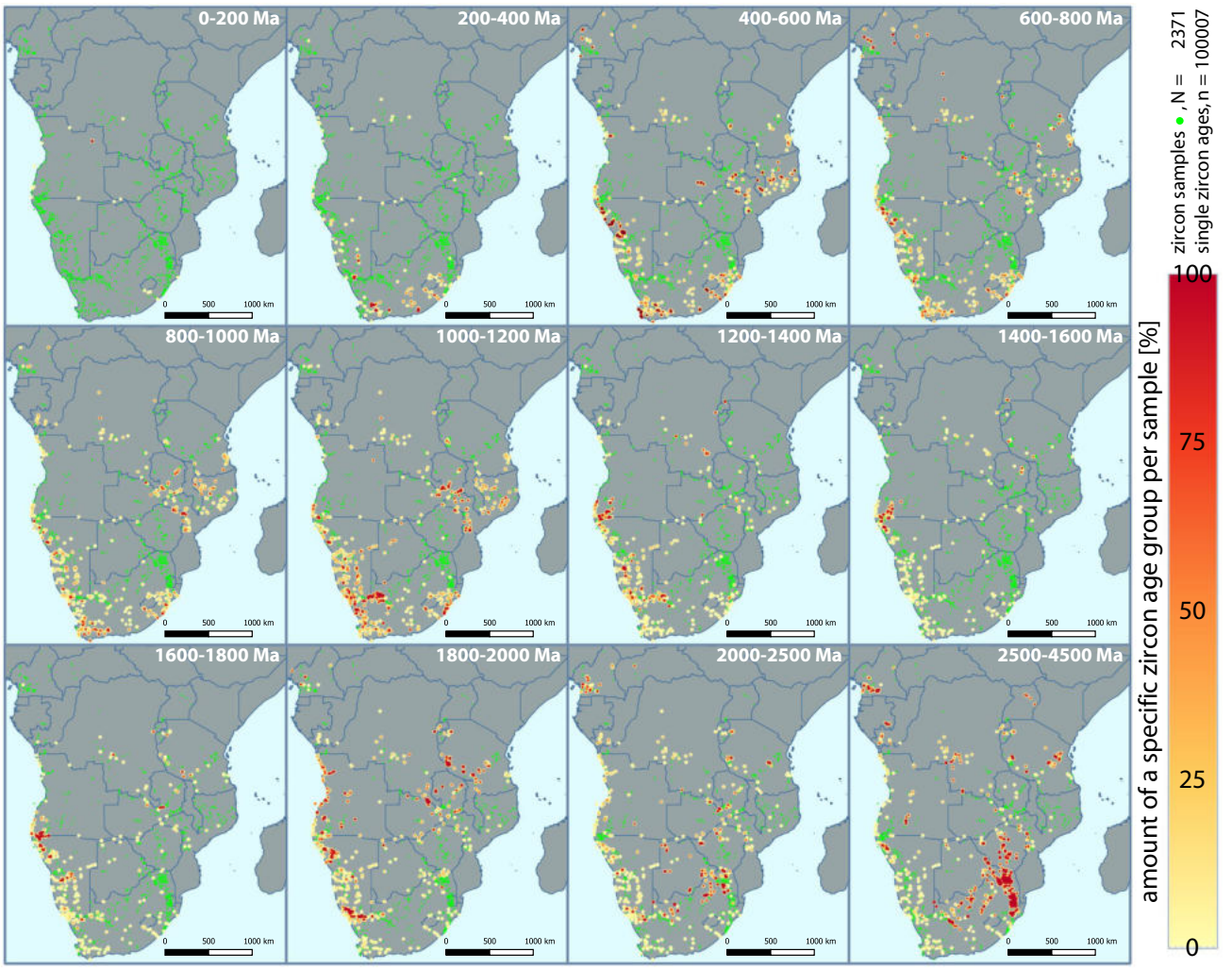

Fig. 8 Spatial distribution of selected zircon ages in southern Africa expressed as a heat map indicating the amount of zircon per sample formed during a specific period of time (as indicated in the upper right of each box). The data were compiled from the literature given in Tab. S4. A colour version of this figure is available in the online edition of this article

no igneous or other source rocks for zircon of this age in the entire Orange catchment, except for the upper reaches of the Orange including the Caledon River that can account for the large sub-peak at its mouth (Fig. 8). Furthermore, Klama (2008) showed that the Cambrian-Ediacaran zircon populations are absent in the middle and lower reaches of the Orange River, which is compatible with the generally accepted ages of the geologic units along the rivers' course (Fig. 2). Accordingly, a long-distance transport of such zircon from the upper reaches is very unlikely. The Hf-isotope composition of zircon from sample NAM-O-18 shows a wide spread of εHf values, which indicates a mixing (Gerdes and Zeh 2006) of Archaean and almost juvenile crustal components (Fig. 6). Although the Hf-data of Klama (2008) show a generally similar trend, most grains of the samples from the upper Orange River cluster in an array between − 5 and + 5 εHf units. This further corroborates the hypothesis that the pan-African zircon grains at the Orange River's mouth do not stem from its upper reaches. But which alternative sources could be taken into account? A potential source is the Fish River, which derives a similar amount of pan-African detrital zircon as found in the lower reaches of the Orange River (samples NAM-O-4 and NAM-O-8, Fig. 5). The Cambrian-Ediacaran zircon grains of the Fish River are rounded (mean roundness ca. 6.1), which is not completely in line with well-rounded zircons of the same age range in the Orange River (mean roundness > 7), but indicates longer transport or intense recycling of these grains. As these differences may result from statistical reasons (< 100 grains for each group), this characteristic should not be over interpreted. Although overlapping in large parts, the spread of εHf values in detrital zircon is smaller in the one analysed sample from the Fish (NAM-O-8) than in the one sample from the Orange River (NAM-O-18; Fig. 6). However, Hf-data reported from the Nama Group (Andersen et al. 2018b) covers the same range of εHf values as the modern Orange River sand. Therefore, it is possible that a certain amount of the Cambrian–Ediacaran zircon of the lower Orange derived from the north via the Fish River and its tributaries. Another potential source of Cambrian–Ediacaran zircon in the lower Orange River is located to the south: the Saldania Belt (e.g. Andersen et al. 2018b; Chemale et al. 2010; Clemens et al. 2017). Here, particularly those parts of the belt that drain to the Atlantic Benguela Current have a high potential to deliver detrital material via coast-parallel inner shelf-transport (de Decker 1988)—including possible short-distance aeolian transport on land—to the north. Pan-African zircon grains of the Saldania Belt show εHf values between ca. -30 and + 5 (Farina et al. 2014; Frimmel et al. 2013; Villaros et al. 2012), which is approximately the range found in sample NAM-O-18 of the lower Orange River. The example of the Cambrian–Ediacaran zircon population that seems to be added to the Orange River detrital signature just at its lowermost reaches—and, therefore, does not reflect any signal from the continental hinterland—highlights the complexity of sediment transport even in regions that were previously considered well known. Thus, some sediments that are transported by the Orange sand highway (Garzanti et al. 2017a) may have their origin even further south than previously expected.

Most detrital zircon grains in the Namib Erg lie within the age spread of the detrital zircon grains occurring in the lowermost reaches of the Orange River (Fig. 9). As postulated by Bluck et al. (2007), Garzanti et al. (2017b), Ribas et al. (2013) and Ward (1989) major parts of the modern Namib Erg seem to have been formed from sands similar to those derived by the Orange River. The newly obtained detrital zircon data corroborate this hypothesis at least for the western parts of the Namib Erg. Nevertheless, either multi-dimensional scaling of the available data (Fig. 9) or simple comparison of the zircon age distribution curves (Fig. 5) reveal some differences, particularly in those samples that are close to the Great Escarpment (e.g. NAMA038, NAMA041). This is in line with observations reported by Corbett (2018), who showed that alluvial fans of the Great Escarpment also provide considerable amounts of siliciclastic sediments to the eastern parts of the Namib and that

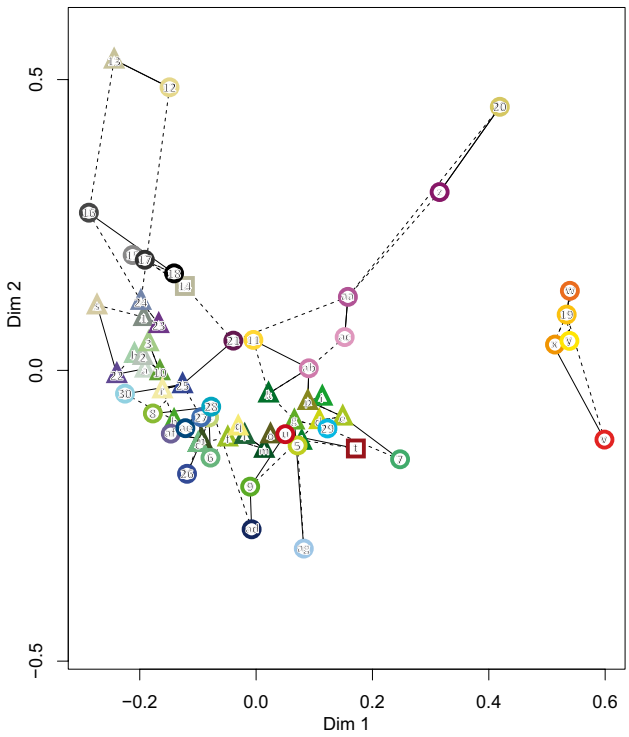

Fig. 9 Non-metric multi-dimensional scaling (MDS) plots after Vermeesch (2013) revealing similarities between samples of Namibian modern sands as already shown in Fig. 5 (symbols and labelling are the same as in Fig. 5). A colour version of this figure is available in the online edition of this article

sediments of mixed sources predominate the central parts of this desert.

Approaching the mouth of the Swakop-Khan catchment, the proposed Orange sand highway of Garzanti et al. (2017a) has significant amounts of or is even overprinted by Damaran detritus. This can be deduced from the zircon morphology, as described above, and is also recorded by the detrital zircon age patterns. The latter show high amounts of Cambrian-Ediacaran (ca. 490–560 Ma) detrital zircon grains with little Tonian–Stenian (ca. 950–1060 Ma) and Orosirian (~ 1900–2050 Ma) age populations. Remarkably, the amount of pre-Ediacaran detrital zircon increases up-stream of the Swakop River, which coincides with the presence of coeval basement inliers as described, e.g. by Longridge et al. (2018). The almost exclusive input of Damaran detritus allows a clear distinction between sands of the Swakop system and those of the Namib Erg (Fig. 9). The input of Damaran detritus by the Swakop River is so dominant that it constitutes the largest parts of beach sands at least up to about 100 km N of the Swakop River's mouth at Henties Bay (sample NAMA051, Fig. 5). In coastal dunes at this locality, another detrital signal is recognised (sample NAMA052). Hence, the aeolian transport of material with Swakop River provenance from the west (i.e. the beach) or the south is negligible compared to coast-parallel transport processes. As the material of the coastal dunes at Henties Bay is very similar to that of the lower Ugab River (Fig. 9), it has to be assumed that material from the Omaruru or Ugab rivers is transported to the shoreline by high velocity winds during the winter months (Ward and Bulley 1988). Beside a main Cambrian-Ediacaran (ca. 490–560 Ma) peak and some scattered Mesoproterozoic ages, there is a distinct Lower Cretaceous peak around ca. 130 Ma in NAMA052. The latter is coeval with magmatism in the Erongo (Wigand et al. 2004), Brandberg (Armstrong et al. 1997; Schmitt et al. 2000), Messum and several smaller complexes (Milner et al. 1995) that lie (partly) within or close to the Omaruru catchment in the NNE to NE of the dune. Two hypotheses can be deduced from these two samples: I) The Orange sand highway (Garzanti et al. 2017a) is at least locally interrupted or masked by sediments of the Swakop River, and II) a certain amount of material of the coastal dunes near Henties Bay is derived from north-northeastern to northeastern source rocks.

Samples collected from the northern Namibian rivers, such as Okavango, Cuando and Zambezi, show also a quite similar detrital zircon age distribution pattern, which is distinct from those of the other regions (Gärtner et al. 2014; Figs. 5; 9). Characterised by Cambrian–Ediacaran (approximately 500–620 Ma), Stenian (ca. 1020–1150 Ma) and Orosirian (~ 1850–2000 Ma) main peaks, these sediments are thought to originate from (multiply?) recycled (Gärtner et al. 2014) and thus, likely homogenised material of the northern Kalahari Basin. The realm of these detrital zircon age patterns seems to be sharply limited to the south and the west. This is indicated by sample NAMA062 and is interpreted to represent mostly local detrital zircon age signals. Additionally, sample NAMA099 shows Damara affinities (Fig. 9) and, therefore, has at least a certain component of southern provenance. "Near steady state" erosion rates of about 5 m • Ma^{-1} have been proposed for the northern flank of the Damara Orogen (Matmon et al. 2018). Hence, the increase of Damara-type detritus to the south of the northern Namibian Rivers shows that the average erosion rate and formation of loose sand is currently slightly higher in the Damara Orogen than in the northern Kalahari Basin.

Such higher erosion rates result in a bias of derived detrital material and are likely mainly triggered by steeper average hill slope angles (Bierman and Caffee 2001; Codilean et al. 2008), at least in arid environments. A further result of locally higher erosion rates are abrupt transitions from a certain detrital zircon signal to another within the same catchment. This is exemplarily shown in the Ugab River, where a rapid change from a Palaeoproterozoic (ca. 1850–1920 Ma) basement to a Damara Orogen detrital zircon age signal, which is characterised by almost pure Cambrian–Ediacaran (ca. 480–560 Ma) zircon age populations, is recorded. There, samples NAMA055 and NAMA057 differ significantly although being sampled only about 150 km away from each other within the main channel of the Ugab River (Fig. 5a). Such massive sediment inputs from areas with higher erosion rates mask the detrital signals coming from other parts of a certain catchment area, irrespective of their size. This is a factor that has to be considered next to preparation-induced bias (Sláma and Košler 2012), zircon fertility of the host rocks (Moecher and Samson 2006) and natural bias induced by hydrodynamic fractionation (Augustson et al. 2018), metamictisation (Markwitz et al. 2017), etc. when analysing and interpreting provenance of sediments. The examples from modern Ugab and also Orange River sands (see above) clearly indicate that the information of river sands sampled at their mouths do not necessarily represent the entire catchment area.

Last the "least complicated" detrital zircon age distribution patterns clearly highlight that sediments derived by the Kunene River (Gärtner et al. 2014; Garzanti et al. 2017a), or found in its vicinity (this study), show a zircon age distribution with particularly high amounts of Mesoproterozoic, ca. 1300–1600 Ma old zircon grains that seem to be extremely rare in entire southern Africa (Fig. 8). Thus, samples that are somehow connected with the Epupa (e.g. Kröner et al. 2015; Seth et al. 2003; 2005) and Kunene Anorthosite complexes (Baxe 2007; Bybee et al. 2019; Lehmann et al. 2020) can easily be distinguished from almost all other samples reported from the Congo and Kalahari Cratons (Fig. 5; Fig. 9). Such zircon grains are a very useful marker population for a potential detrital component of Epupa or Kunene

Anorthosite complex origin if occurring abundantly (e.g. samples S3938 of Garzanti et al. 2017a and NAMA062 of this study).

Summarising the data, the main route of sediment transport along the Namibian coast is from the south to the north with an assumed high input from the Orange River. However, detrital zircon data also allow the possibility that the so called Orange sand highway (Garzanti et al. 2017a) originates further south or potentially derives large amounts of sand from the erosion of the Nama Basin and adjacent areas via the Fish River. Persistent winds from the south trigger aeolian transport from the coast to the western parts of the Namib Erg, while its eastern parts are fed from sources around the Great Escarpment. These patterns of sediment transport turn the Orange sand highway into the Southern Namibian Sediment Vortex (SNSV), which is locked to the north by the Damara Orogen. The flux of material from the south is abruptly diluted by high proportions of Damaran detritus at the mouth of the Swakop River, whereas the influence of aeolian transport from coast-parallel transported sediments to the hinterland drops to very low levels further north. There, sediments are blown from the river beds of perennial rivers like Omaruru and Ugab towards the coast by winds from northwest. Any sediment movement from the south to the north ends up in southern Angola (Garzanti et al. 2017a). Remarkably, the unique detrital zircon signal of the Kunene River and its tributaries seems to be limited to the close vicinity of the Kunene Intrusive and Epupa complexes and thus, can be used as excellent provenance marker of this area. Inland, the Damara Orogen represents the main factor for sediment formation and their distribution due to slightly higher erosion rates than in the surrounding landscape. Finally, the northern Namibian rivers, like the Okavango and Zambezi, form a separate system that redistributes the sediments of the northern Kalahari Basin towards the east and southeast (Gärtner et al. 2014) to form the Okavango Delta and supply sediments to the Zambezi flats prior to the Victoria Falls (van der Lubbe et al. 2016).

Conclusions

Owing to its almost ubiquitous occurrence, resistance against physical and chemical weathering and datability, zircon grains of various sedimentary archives are widely used for palaeogeographic and palaeoclimatic reconstructions. Although this study only provides initial data, it becomes clear that a combination of easy-to-log detrital zircon morphology and state-of-the-art geochronologic techniques in combination with comprehensive geo-databases allows obtaining more detailed models of sediment transport than commonly used monomethod approaches. Particularly in regions that host several geotectonic realms characterised by very similar, repetitively occurring zircon age spectra with assumed high ratios of sediment recycling and homogenisation, like Namibia, the need for further proxies allowing

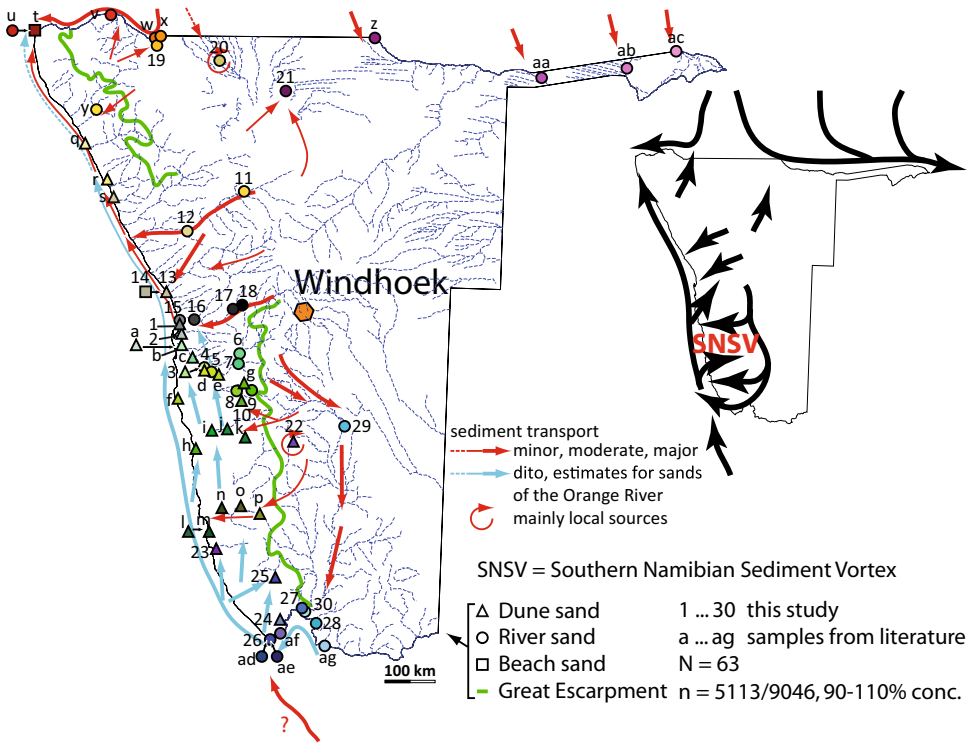

Fig. 10 Main routes of modern sediment transport in Namibia. The small inset in the upper right shows a simplified visualisation of the main fluxes of modern sediment and highlights the Southern Namibian Sediment Vortex (SNSV). A colour version of this figure is available in the online edition of this article

discrimination becomes obvious. Therefore, the interpretation of newly obtained data reveals potential sources, traps and routes of modern sediment transport even for less-studied regions of Namibia. Combining all data obtained in this and previously published studies, a first sketch of the complex modern sediment transport in Namibia can be drawn as proposed in Fig. 10. This initial approach proposes to expand or complement the concept of the Orange sand highway by a Southern Namibian Sediment Vortex (SNSV). The still existing uncertainties concerning modern sediment transport in a very well-studied region with entirely known climatic, geologic and geomorphologic factors highlight the necessity of much more research to reconstruct past environments with even less accuracy.

Supplementary Information The online version contains supplementary material available at https://doi.org/10.1007/s00531-021-02146-1.

Acknowledgements This study is part of project No. LI 521/32-1 "Evolution of the western Namibian drainage systems since Eocene times – a multi-methodical approach" Granted by the German Science Foundation (DFG). The authors like to thank Wladyslaw Altermann and an anonymous reviewer for the comments and suggestions that substantially helped to improve the manuscript.

Funding Open Access funding enabled and organized by Projekt DEAL. This study is part of project No. LI 521/32–1 "Evolution of the western Namibian drainage systems since Eocene times – a multi-methodical approach" granted by the German Science Foundation (DFG).

Data availability All data of this study can be found in the online resources to this article on the publisher's web-site.

Code availability Does not apply.

Declarations

Conflict of interest The authors declare that they have no known competing financial interests or personal relationships that could have appeared to influence the work reported in this paper.

References

Aleinikoff JN, Muhs DR, Bettis EA, Johnson WC, Fanning CM, Benton R (2008) Isotopic evidence for the diversity of late Quaternary loess in Nebraska: glaciogenic and nonglaciogenic sources. GSA Bull 120(11/12):1362–1377. https://doi.org/10.1130/B26222.1

Andersen T, Kristoffersen M, Elburg MA (2018a) Visualizing, interpreting and comparing detrital zircon age and Hf isotope data in basin analysis—a graphical approach. Basin Res 30:132–147. https://doi.org/10.1111/bre.12245

Andersen T, Elburg MA, van Niekerk HS, Ueckermann H (2018b) Successive sedimentary recycling regimes in southwestern Gondwana: evidence from detrital zircons in Neoproterozoic to Cambrian sedimentary rocks in southern Africa. Earth-Sci Rev 181:43–60. https://doi.org/10.1016/j.earscirev.2018.04.001

Armstrong RA, McDougall I, Watkins RT (1997) U/Pb zircon ages of Damaraland complexes, Namibia. EOS Trans Am Geophys Union 78:742

Atlas of Namibia Project (2002) Grass cover in Namibia (map, 1:7,500,000). Directorate of Environmental Affairs, Namibia Ministry of Environment and Tourism, as provided by the Digital Atlas of Namibia hosted by the University of Cologne. http://www.uni-koeln.de/sfb389/e/e1/download/atlas_namibia/e1_download_living_resources_e.htm (Accessed 30 July 2018).

Augustson C, Voigt T, Bernhart K, Kreißler M, Gaupp R, Gärtner A, Hofmann M, Linnemann U (2018) Zircon size-age sorting and source-area effect: The German triassic buntsandstein group. Sed Geol 375:218–231. https://doi.org/10.1016/j.sedgeo.2017.11.004

Bailie R, Rajesh HM, Gutzmer J (2012) Bimodal volcanism at the western margin of the Kaapvaal Craton in the aftermath of collisional events during the Namaqua-Natal Orogeny: the Koras Group, South Africa. Precambrian Res 200–203:163–183. https://doi.org/10.1016/j.precamres.2012.01.017

Barnes J (1999) Barchan dune morphology, migration and management on the Kuiseb River delta, Namibia. MSc thesis, Oxford University

Baxe OSS (2007) Geocronologia de Complexos Máfico-Ultramáficos: Exemplo da Série Superior do Complexo de Niquelândia, Brasil, e do Complexo Kunene, Angola. MSc thesis, Universidade de Brasília

Begg GC, Griffin WL, Natapov LM, O'Reilly SY, Grand SP, O'Neill CJ, Hronsky JMA, Poudjom Djomani Y, Swain CJ, Deen T, Bowden P (2009) The lithospheric architecture of Africa: seismic tomography, mantle petrology, and tectonic evolution. Geosphere 5:23–50. https://doi.org/10.1130/GES00179.1

Bierman PR, Caffee M (2001) Slow rates of rock surface erosion and sediment production across the Namib Desert and Escarpment, southern Africa: American. J Sci 301:326–358. https://doi.org/10.2475/ajs.301.4-5.326

Bluck BJ, Ward JD, Cartwright J, Swart R (2007) The Orange River, southern Africa: an extreme example of a wave-dominated sediment dispersal system in the South Atlantic Ocean. J Geol Soc London 164:341–351. https://doi.org/10.1144/0016-76492005-189

Blum M, Pecha M (2014) Mid-cretaceous to Paleocene North American drainage reorganization from detrital zircons. Geology 42(7):607–610. https://doi.org/10.1130/G35513.1

Bónová K, Pańczyk M, Bóna J (2020) Surface microtextures and new U-Pb dating of detrital zircons from the Eocene Strihovice sandstones in the Magura Nappe of the External Western Carpathians: implications for their provenance. Int J Earth Sci 109:1565–1587. https://doi.org/10.1007/s00531-020-01859-z

Bouvier A, Vervoort JD, Patchett PJ (2008) The Lu-Hf and Sm-Nd isotopic composition of CHUR: constraints from unequilibrated chondrites and implications for the bulk composition of terrestrial planets. Earth Planet Sci Lett 273:48–57. https://doi.org/10.1016/j.epsl.2008.06.010

Burger AJ, Walraven T (1976) Summary of age determinations carried out during the period April 1975 to March 1976. Ann Geol Surv South Afr 11:323–329

Burrough SL, Thomas DSG (2013) Central southern Africa at the time of the African Humid Period: a new analysis of Holocene palaeoenvironmental and palaeoclimate data. Quat Sci Rev 80:29–46. https://doi.org/10.1016/j.quascirev.2013.08.001

Bybee GM, Hayes B, Owen-Smith TM, Lehmann J, Ashwal LD, Brower AM, Hill CM, Corfu F, Manga M (2019) Proterozoic massif-type anorthosites as the archetypes of long-lived (≥ 100 Myr) magmatic systems—new evidence from the Kunene Anorthosite Complex (Angola). Precambrian Res 332:105393. https://doi.org/10.1016/j.precamres.2019.105393

Cantine MD, Setera JB, VanTongeren JA, Mwinde C, Bergmann KD (2020) Grain size and transport biases in an Ediacaran detrital zircon record. Essoar. https://doi.org/10.1002/essoar.10504412.1

Caputo MV, Soares EAA (2016) Eustatic and tectonic change effects in the reversion of the transcontinental Amazon River drainage system. Braz J Geol 46(2):301–328. https://doi.org/10.1590/2317-4889201620160066

De Carvalho H, Tassinari C, Alves PH, Guimarães F, Simões MC (2000) Geochronological review of the Precambrian in western Angola: links with Brazil. J Afr Earth Sci 31:383–402. https://doi.org/10.1016/S0899-5362(00)00095-6

Catuneanu O, Wopfner H, Eriksson PG, Cairncross B, Rubidge BS, Smith RMH, Hancox PJ (2005) The Karoo basins of south-central Africa. J Afr Earth Sci 43:211–253. https://doi.org/10.1016/j.jafrearsci.2005.07.007

Chauvel C, Lewin E, Carpentier M, Arndt NT, Marini JC (2008) Role of recycled oceanic basalt and sediment in generating the Hf-Nd mantle array. Nat Geosci 1:64–67. https://doi.org/10.1038/ngeo.2007.51

Chemale F Jr, Scheepers R, Gresse PG, Van Schmus WR (2010) Geochronology and sources of late Neoproterozic to Cambrian granites of the Saldania Belt. Int J Erath Sci 100:431–444. https://doi.org/10.1007/s00531-010-0579-1

Clemens JD, Buick IS, Frei D, Lana C, Villaros A (2017) Post-orogenic shoshonitic magmas of the Yzerfontein pluton, South Africa: the 'smoking gun' of mantle melting and crustal growth during Cape granite genesis? Contrib Mineral Petrol 172:72. https://doi.org/10.1007/s00410-017-1390-9

Codilean AT, Bishop P, Stuart FM, Hoey TB, Fabel D, Freeman SPHT (2008) Single-grain cosmogenic ^{21}Ne concentrations in fluvial sediments reveal spatially variable erosion rates. Geology 36(2):159–162. https://doi.org/10.1130/G24360A.1

Comin-Chiaramonti P, de Min A, Girardi VAV, Ruberti E (2011) Post-paleozoic magmatism in angola and Namibia: a review. Geol Soc Am SP 478:223–248. https://doi.org/10.1130/2011.2478(12)

Corbett I (2018) The influence of the benguela low-level coastal jet on the architecture and dynamics of aeolian transport corridors in the Sperrgebiet, Namibia. Communs Geol Surv Namibia 20:9–58

Cross AJ, Crispe AJ (2007) SHRIMP U-Pb analyses of detrital zircon: a window to understanding the Paleoproterozoic development of the Tanami Region, northern Australia. Mineral Depos 42:27–50. https://doi.org/10.1007/s00126-006-0102-6

Crouvi O, Amit R, Enzel Y, Gillespie AR (2010) Active sand seas and the formation of desert loess. Quat Sci Rev 29:2087–2098. https://doi.org/10.1016/j.quascirev.2010.04.026

Dansie AP, Wiggs GFS, Thomas DSG, Washington R (2017) Measurements of windblown dust characteristics and ocean fertilization potential: the ephemeral river valleys of Namibia. Aeolian Res 29:30–41. https://doi.org/10.1016/j.aeolia.2017.08.002

De Decker RH (1988) The wave regime on the inner shelf south of the Orange River and its implications for sediment transport. S-Afr Tydskr Geol 91(3):358–371

De Waele B, Fitzsimmons ICW (2007) The nature and timing of Palaeoproterozoic sedimentation at the southeastern margin of the Congo Craton; zircon U-Pb geochronology of plutonic, volcanic and clastic units in northern Zambia. Precambrian Res 159:95–116. https://doi.org/10.1016/j.precamres.2007.06.004

De Waele B, Fitzsimons ICW, Wingate MTD, Tembo F, Mapani B, Belousova EA (2009) The geochronological framework of the Irumide Belt: a prolonged crustal history along the margin of the Bangweulu Craton. Am J Sci 309:132–187. https://doi.org/10.2475/02.2009.03

Dhuime B, Hawkesworth C, Cawood P (2011) When continents formed. Science 331(6014):154–155. https://doi.org/10.1126/science.1201245

Drüppel K, Littmann S, Romer RL, Okrusch M (2007) Petrology and isotope geochemistry of the Mesoproterozoic anorthosite and related rocks of the Kunene Intrusive Complex, NW Namibia. Precambrian Res 156:1–31. https://doi.org/10.1016/j.precamres.2007.02.005

Dunkl I, Demény A (1997) Exhumation of the rechnitz window at the border of the eastern alps and pannonian basin during neogene extension. Tectonophysics 272:197–211. https://doi.org/10.1016/S0040-1951(96)00258-2

Eglington BM, Armstrong RA (2003) Geochronological and isotopic constraints on the Mesoproterozoic Namaqua-Natal Belt: evidence from deep borehole intersections in South Africa. Precambrian Res 125:179–189. https://doi.org/10.1016/S0301-9268(02)00199-7

Farina F, Stevens G, Gerdes A, Frei D (2014) Small-scale Hf isotopic variability in the Peninsula pluton (South Africa): the processes that control inheritance of source ^{176}Hf/^{177}Hf diversity in S-type granites. Contrib Mineral Petrol 168:1065. https://doi.org/10.1007/s00410-014-1065-8

Fedo CM, Sircombe KN, Rainbird RH (2003) Detrital zircon analysis of the sedimentary record. In: Hanchar JM, Hoskin PWO (eds) Zircon. Rev Min Geochem 53:277–303. https://doi.org/10.1515/9781501509322-013

Fernandez-Alonso M, Cutten H, De Waele B, Tack L, Tahon A, Baudet D, Barritt SD (2012) The Mesoproterozoic Karagwe-Ankole Belt (formerly NE Kibara Belt): the result of prolonged extensional intracratonic basin developement puncutated by two short-lived compressional events. Precambrian Res 216–219:63–86. https://doi.org/10.1016/j.precamres.2012.06.007

Fitch FJ, Miller JA (1984) Dating Karoo igneous rocks by conventional K-Ar and ^{40}Ar/^{39}Ar age spectrum methods. Geol Soc South Afr Spec Pub 13:247–266

Frimmel HE, Tack L, Basei MS, Nutman AP, Boven A (2006) Provenance and chemostratigraphy of the Neoproterozoic West Congolian Group in the Democratic Republic of Congo. J Afr Earth Sci 46:221–239. https://doi.org/10.1016/j.jafrearsci.2006.04.010

Frimmel HE, Basei MAS, Correa VX, Mbangula N (2013) A new lithostratigraphic subdivision and geodynamic model for the Pan-African western Saldania Belt, South Africa. Precambrian Res 231:218–235. https://doi.org/10.1016/j.precamres.2013.03.014

Ganbat A, Tsujimori T, Boniface N, Pastor-Galán D, Aoki S, Aoki K (2021) Crustal evolution of the Paleoproterozoic Ubendian Belt (SW Tanzania) western margin: a Central African Shield amalgamation tale. Gondwana Res 91:286–306. https://doi.org/10.1016/j.gr.2020.12.009

Gärtner A (2011) Morphologische, geochronologische und isotopengeochemische Untersuchungen an rezenten Sedimenten der Elbe. Diploma thesis, Technische Universität Dresden

Gärtner A, Linnemann U, Sagawe A, Hofmann M, Ullrich B, Kleber A (2013) Morphology of zircon crystal grains in sediments—characteristics, classifications, definitions. Geol Saxon 59:65–73

Gärtner A, Linnemann U, Hofmann M (2014) The provenance of northern Kalahari Basin sediments and growth history of the southern Congo Craton reconstructed by U-Pb ages of zircons from recent

river sands. Int J Earth Sci 103:579–595. https://doi.org/10.1007/s00531-013-0974-5
Gärtner A, Toto Nienguesso AB, Linnemann U, Hofmann M, Gerdes A, Marko L, Krause R, Lana C, Makenda A (2016) U-Th-Pb and Hf isotopic studies of zircon from the West Congo Belt of NW Angola and the adjacent igneous basement. IGC 35:2501
Gärtner A, Youbi N, Villeneuve M, Sagawe A, Hofmann M, Mahmoudi A, Boumehdi MA, Linnemann U (2017) The zircon evidence of temporally changing sediment transport—the NW Gondwana margin during Cambrian to Devonian time (Aoucert and Smara areas, Moroccan Sahara). Int J Earth Sci 106:2747–2769. https://doi.org/10.1007/s00531-017-1457-x
Gärtner A, Youbi N, Villeneuve M, Linnemann U, Sagawe A, Hofmann M, Zieger J, Mahmoudi A, Boumehdi MA (2018) Provenance of detrital zircon from siliciclastic rocks of the Sebkha Gezmayet unit of the Adrar Souttouf Massif (Moroccan Sahara)—Palaeogeographic implications. C R Geosci 350(6):255–266. https://doi.org/10.1016/j.crte.2018.06.004
Gärtner A, Merchel S, Niedermann S, Braucher R, ASTER-Team, Steier P, Rugel G, Scharf A, Le Bras L, Linnemann U (2020) Nature does the averaging—in-situ produced ^{10}Be, ^{21}Ne, and ^{26}Al in a Very Young River Terrace. geosciences 10:237. https://doi.org/10.3390/geosciences10060237
Garzanti E, Andò S, Vezzoli G (2008) Settling equivalence of detrital minerals and grain-size dependence of sediment composition. Earth Planet Sci Lett 273:138–151. https://doi.org/10.1016/j.epsl.2008.06.020
Garzanti E, Vermeesch P, Ando S, Lustrino M, Padoan M, Vezzoli G (2014a) Ultra-long distance littoral transport of Orange sand and provenance of the Skeleton Coast Erg (Namibia). Mar Geol 357:25–36. https://doi.org/10.1016/j.margeo.2014.07.005
Garzanti E, Vermeesch P, Padoan M, Resentini A, Vezzoli G, Andò S (2014b) Provenance of Passive-Margin Sand (Southern Africa). J Geol 122:17–42. https://doi.org/10.1086/674803
Garzanti E, Dinis P, Vermeesch P, Andò S, Hahn A, Huvi J, Limonta M, Padoan M, Resentini A, Rittner M, Vezzoli G (2017a) Sedimentary processes controlling ultralong cells of littoral transport: Placer formation and termination of the Orange sand highway in southern Angola. Sedimentology 65(2):431–460. https://doi.org/10.1111/sed.12387
Garzanti E, Dinis P, Vermeesch P, Andò S, Hahn A, Huvi J, Limonta M, Padoan M, Resentini A, Rittner M, Vezzoli G (2017b) Dynamic uplift, recycling, and climate control on the petrology of passive-margin sand (Angola). Sed Geol 375:86–104. https://doi.org/10.1016/j.sedgeo.2017.12.009
Geological Survey of Namibia (1977) Geological Map of Namibia 1:250000 Geological Series, Sheet 2416 Mariental.Geological Survey of Namibia, 1994. Geological Map of Namibia 1:250000 Geological Series, Sheet 2314 Kuiseb
Geological Survey of Namibia (1994) Geological Map of Namibia 1:250000 Geological Series, Sheet 2314 Kuiseb
Geological Survey of Namibia (2000) Geological Map of Namibia 1:250000 Geological Series, Sheet 2516 Gibeon
Gerdes A, Zeh A (2006) Combined U-Pb and Hf isotope LA-(MC-)ICP-MS analyses of detrital zircons: Comparison with SHRIMP and new constraints for the provenance and age of an Armorican metasediment in Central Germany. Earth Planet Sci Lett 249:47–61. https://doi.org/10.1016/j.epsl.2006.06.039
Gerdes A, Zeh A (2009) Zircon formation versus zircon alteration: new insights from combined U-Pb and Lu-Hf in situ LA-ICPMS analyses, and consequences for the interpretation of Archean zircon from the Central Zone of the Limpopo Belt. Chem Geol 261:230–243. https://doi.org/10.1016/j.chemgeo.2008.03.005
Glynn SM, Master S, Wiedenbeck M, Davis DW, Kramers JD, Belyanin GA, Frei D, Oberthür T (2017) The Proterozoic Choma-Kalomo Block, SE Zambia: exotic terrane or reworked segment of the Zimbabwe Craton? Precambrian Res 298:421–438. https://doi.org/10.1016/j.precamres.2017.06.020
Gong X, Knorr G, Lohmann G, Zhang X (2013) Dependence of abrupt Atlantic meridional ocean circulation changes on climate background states. Geophys Res Lett 40:3698–3704. https://doi.org/10.1002/grl.50701
Goosmann EA, Catling DC, Som SM, Altermann W, Buick R (2018) Eolianite grain size distributions as a proxy for large changes in planetary atmospheric density. J Geophys Res Planets 123:2506–2526. https://doi.org/10.1029/2018JE005723
Goscombe B, Foster DA, Gray D, Wade B (2018) The evolution of the damara orogenic system: a record of west gondwana assembly and crustal response. In: Siegesmund S, Basei MAS, Oyhatçabal P (eds) Geology of Southwest Gondwana. Regional Geol Rev 303–352. https://doi.org/10.1007/978-3-319-68920-3_12
Greenbaum N, Schwartz U, Benito G, Porat N, Cloete GC, Enzel Y (2014) Paleohydrology of extraordinary floods along the Swakop River at the margin of the Namib Desert and their paleoclimate implications. Quat Sci Rev 103:153–169. https://doi.org/10.1016/j.quascirev.2014.08.021
Gyory J, Bischof B, Mariano AJ, Ryan EH (2004) The angola current. Ocean Surface Currents. http://oceancurrents.rsmas.miami.edu/atlantic/angola.html (Accessed 30 July 2018)
Haddon IG, McCarthy TS (2005) The Mesozoic-Cenozoic interior sag basins of Central Africa: the Late-Cretaceous–Cenozoic Kalahari and Okavango basins. J Afr Earth Sci 43:316–333. https://doi.org/10.1016/j.jafrearsci.2005.07.008
Hastie WW, Watkeys MK, Aubourg C (2014) Magma flow in dyke swarms of the Karoo LIP: implications for the mantle plume hypothesis. Gondwana Res 25:736–755. https://doi.org/10.1016/j.gr.2013.08.010
Hauzenberger CA, Tenczer V, Bauernhofer A, Fritz H, Klötzli U, Košler J, Wallbrecher E, Muhongo S (2014) Termination of the Southern irumide belt in Tanzania: Zircon U/Pb geochronology. Precambrian Res 255:144–162. https://doi.org/10.1016/j.precamres.2014.09.021
Hipondoka MHT, Mauz B, Kempf J, Packman S, Chiverrell RC, Bloemendal J (2014) Chronology of sand ridges and the late quaternary evolution of the Etosha Pan, Namibia. Geomorphology 204:553–563. https://doi.org/10.1016/j.geomorph.2013.08.034
Hofmann M, Linnemann U, Hoffmann K-H, Gerdes A, Eckelmann K, Gärtner A (2013) The Namuskluft and Dreigratberg sections in southern Namibia (Kalahari Craton, Gariep Belt): a geological history of Neoproterozoic rifting and recycling of cratonic crust during the dispersal of Rodinia until the amalgamation of Gondwana. Int J Earth Sci 103:1187–1202. https://doi.org/10.1007/s00531-013-0949-6
Hofmann M, Linnemann U, Hoffmann K-H, Germs G, Gerdes A, Marko L, Eckelmann K, Gärtner A, Krause R (2015) The four Neoproterozoic Glaciations of southern Namibia and their detrital zircon record: the fingerprints of four crustal growth events during two supercontinent cycles. Precambrian Res 259:176–188. https://doi.org/10.1016/j.precamres.2014.07.021
Houben G, Kaufhold S, Miller RMcG, Lohe C, Hinderer M, Noll M, Hornung J, Joseph R, Gerdes A, Sitnikova M, Quniger M (2020) Stacked megafans of the Kalahari Basin as archives of paleogeography, river capture, and Cenozoic peleoclimate of southwestern Africa. J Sed Res 90:980–1010. https://doi.org/10.2110/jsr.2020.46
Iizuka T, Campbell IH, Allen CM, Gill JB, Maruyama S, Makoka F (2013) Evolution of the African continental crust as recorded by U-Pb, Lu–Hf and O isotopes in detrital zircons from modern rivers. Geochim Cosmochim Acta 107:96–120. https://doi.org/10.1016/j.gca.2012.12.028

Jackson SE, Pearson NJ, Griffin WL, Belousova EA (2004) The application of laser ablation-inductively coupled plasma-mass spectrometry to in situ U-Pb zircon geochronology. Chem Geol 211:47–69. https://doi.org/10.1016/j.chemgeo.2004.06.017

Jacobs J, Pisarevsky S, Thomas RJ, Becker T (2008) The Kalahari Craton during the assembly and dispersal of Rodinia. Precambrian Res 160:142–158. https://doi.org/10.1016/j.precamres.2007.04.022

Jelsma HA, Vinyu ML, Valbracht PJ, Davies GR, Wijbrans JR, Verdurmen EAT (1996) Constraints on Archaean crustal evolution of the Zimbabwe craton: a U-Pb zircon, Sm-Nd and Pb-Pb whole rock isotope study. Contrib Mineral Petrol 124:55–70. https://doi.org/10.1007/s004100050173

Jelsma HA, McCourt S, Perritt SH, Armstrong RA (2018) The geology and evolution of the angolan shield, Congo Craton. In: Siegesmund S, et al. (eds) Geology of southwest gondwana, Regional Geol Rev 217–239. https://doi.org/10.1007/978-3-319-68920-3_9

Jiang Q, Yang X (2019) Sedimentological and geochemical composition of aeolian sediments in the taklamakan desert: implications for provenance and sediment supply mechanisms. J Geophys Res Earth Surf 124:1217–1237. https://doi.org/10.1029/2018JF004990

Kabete JM, McNaughton NJ, Groves DI, Mruma AH (2012) Reconnaissance SHRIMP U-Pb zircon geochronology of the Tanzania Craton: evidence for Neoarchaean granitoid-greenstone belts in the Central Tanzania Region and the South East African Orogen. Precambrian Res 216–219:232–266. https://doi.org/10.1016/j.precamres.2012.06.020

Kaseke KF, Wang L, Wanke H, Turewicz V, Koeniger P (2016) An analysis of precipitation isotope distributions across namibia using historical data. PLoS ONE. https://doi.org/10.1371/journal.pone.0154598

Kempe U, Bombach K, Matukov D, Schlothauer T, Hutschenreuter J, Wolf D, Sergeev S (2004) Pb/Pb and U/Pb zircon dating of subvolcanic rhyolite as a time marker for Hercynian granite magmatism and Sn mineralisation in the Eibenstock granite, Erzgebirge, Germany: Considering effects of zircon alteration. Mineral Depos 39:646–669. https://doi.org/10.1007/s00126-004-0435-y

Klama KO (2008) U-Pb Geochronologie, Hf Isotopie und Spurenelementgeochemie detritischer Zirkone aus rezenten Sedimenten des Orange- und Vaal River Flusssystems in Südafrika. Doctoral Thesis, University of Frankfurt/Main

Kleinhanns IC, Fullgraf T, Wilsky F, Nolte N, Fliegel D, Klemd R, Hansen BT (2015) U-Pb zircon ages and (isotope) geochemical signatures of the Kamanjab Inlier (NW Namibia): constraints on Palaeoproterozoic crustal evolution along the southern Congo craton. Geol Soc London SP 389:165–195. https://doi.org/10.1144/SP389.1

Kokonyangi JW, Kampunzu AB, Armstrong R, Arima M, Yoshida M, Okudaira T (2007) U-Pb SHRIMP dating of detrital zircons from the Nzilo Group (Kibaran Belt): implications for the source sediments and mesoproterozoic evolution of Central Africa. J Geol 115:99–113. https://doi.org/10.1086/509270

Köksal S, Cemal Göncüoglu M, Toksoy-Köksal F, Möller A, Kemnitz H (2008) Zircon typologies and internal structures as petrogenetic indicators in contrasting granitoid types from central Anatolia, Turkey. Mineral Petrol 93:185–211. https://doi.org/10.1007/s00710-007-0228-y

Konopásek J, Hoffmann K-H, Sláma J, Košler J (2017) The onset of flysch sedimentation in the Kaoko Belt (NW Namibia)—implications for the pre-collisional evolution of the Kaoko–Dom Feliciano–Gariep orogen. Precambrian Res 298:220–234. https://doi.org/10.1016/j.precamres.2017.06.017

Krinsley DH, Doornkamp JC (2011) Atlas of quartz sand surface textures. Cambridge University Press

Kröner A (1973) Comments on "Is the African plate stationary?" Nature 243:29–30. https://doi.org/10.1038/243029a0

Kröner A, Rojas-Agramonte Y, Wong J, Wilde SA (2015) Zircon reconnaissance dating of Proterozoic gneisses along the Kunene River of northwestern Namibia. Tectonophysics 662:125–139. https://doi.org/10.1016/j.tecto.2015.04.020

Kröner A, Brandl G, Brandt S, Klemd R, Xie H (2018) Geochronological evidence for Archaean and Palaeoproterozoic polymetamorphism in the Central Zone of the Limpopo Belt, South Africa. Precambrian Res 310:320–347. https://doi.org/10.1016/j.precamres.2018.03.013

Lancaster N (1982) Dunes on the Skeleton Coast, Namibia (South West Africa): geomorphology and grain size relationships. Earth Surf Proc Land 7:575–587. https://doi.org/10.1002/esp.3290070606

Lawrence RL, Cox R, Mapes RW, Coleman DS (2011) Hydrodynamic fractionation of zircon age populations. GSA Bull 123(1/2):295–395. https://doi.org/10.1130/B30151.1

Leary RJ, Smith ME, Umhoefer P (2020) grain-size control on detrital zircon cycloprovenance in the late Paleozoic Paradox and Eagle Basins, USA. JGR Solid Earth 125(7):e2019JB019226. https://doi.org/10.1029/2019JB019226

Lehmann J, Bybee GM, Hayes B, Owen-Smith TM, Belyanin G (2020) Emplacement of the giant Kunene AMCG complex into a contractional ductile shear zone and implications for the Mesoproterozoic tectonic evolution of SW Angola. Int J Earth Sci. https://doi.org/10.1007/s00531-020-01837-5

Link PK, Fanning CM, Beranek LP (2005) Reliability and longitudinal change of detrital-zircon age spectra in the Snake River system, Idaho and Wyoming: An example of reproducing the bumpy barcode. Sediment Geol 182:101–142. https://doi.org/10.1016/j.sedgeo.2005.07.012

Linnemann U, Pieren Pidal A, Hofmann M, Drost K, Quesada C, Gerdes A, Marko L, Gärtner A, Zieger J, Ulrich J, Krause R, Vickers-Rich P, Horak J (2017) A ~ 565 Ma old glaciation in the Ediacaran of peri-Gondwanan West Africa. Int J Earth Sci 107(3):885–911. https://doi.org/10.1007/s00531-017-1520-7

Linol B, de Wit MJ, Barton E, Guillocheau F, de Wit MCJ, Colin J-P (2015) Paleogeography and tectono-stratigraphy of carboniferous-permian and triassic 'Karoo-Like' sequences of the Congo Basin. In: de Wit MJ, Guillocheau F, de Wit MCJ (eds) Geology and resource potential of the Congo Basin. Regional Geol Rev, 111–134. https://doi.org/10.1007/978-3-642-29482-2_7

Longridge L, Kinnaird J, Gibson R, Hawkesworth C, Armstrong R (2018) Crustal recycling in the Damara Belt, Namibia, and interaction of the Congo and Kalahari Cratons—evidence from zircon U-Pb, Hf and O isotopes. South Afr J Geol 121(3):237–252. https://doi.org/10.25131/sajg.121.0018

Macey PH, Bailie RH, Miller JA, Thomas RJ, de Beer C, Frei D, le Roux PJ (2018) Implications of the distribution, age and origins of the granites of the Mesoproterozoic Spektakel Suite for the timing of the Namaqua Orogeny in the Bushmanland Subprovince of the Namaqua-Natal Metamorphic Province, South Africa. Precambrian Res 312:68–98. https://doi.org/10.1016/j.precamres.2018.02.026

Markwitz V, Kirkland CL, Mehnert A, Gessner K, Shaw J (2017) 3-D characterization of detrital zircon grains and its implications for fluvial transport, mixing, and preservation bias. Geochem Geophys Geosys 18:4655–4673. https://doi.org/10.1002/2017GC007278

McCourt S, Armstrong RA, Jelsma H, Mapeo RBM (2013) New U-Pb SHRIMP ages from the Lubango region, SW Angola: insights into the Palaeoproterozoic evolution of the Angolan

Shield, southern Congo Craton, Africa. J Geol Soc Lond 170:353–363. https://doi.org/10.1144/jgs2012-059
Middleton NJ (2017) Desert dust hazards: a global review. Aeolian Res 24:53–63. https://doi.org/10.1016/j.aeolia.2016.12.001
Miller RMcG (2008) Namib group. In: Miller RMcG (ed) The geology of Namibia—volume 3 Palaeozoic to Cenozoic 25-1-25-66
Milner SC, Le Roex AP, O'Connor JM (1995) Age of Mesozoic igneous rocks in northwestern Namibia, and their relationship to continental breakup. J Geol Soc London 152:97–104. https://doi.org/10.1144/gsjgs.152.1.0097
Moecher DP, Samson SD (2006) Differential zircon fertility of source terranes and natural bias in the detrital zircon record: Implications for sedimentary provenance analysis. Earth Planet Sci Lett 247:252–266. https://doi.org/10.1016/j.epsl.2006.04.035
Montes C, Cardona A, Jaramillo C, Pardo A, Silva JC, Valencia V, Ayala C, Pérez-Angel LC, Rodriguez-Parra LA, Ramirez V, Niño H (2015) Middle Miocene closure of the Central American Seaway. Science 348(6231):226–229. https://doi.org/10.1126/science.aaa2815
Moore AE, Cotterill FP, Main MP, Williams HB (2007) The Zambezi River. In: Gupta A (ed) Large rivers: geomorphology and management, pp 311–332
Moura CAV, Pinheiro BLS, Nogueira ACR, Gorayeb PSS, Galarza MA (2008) Sedimentary provenance and palaeoenvironment of the Baixo Araguaia Supergroup: constraints on the palaeogeographical evolution of the Araguaia Belt and assembly of West Gondwana. Geol Soc London SP 294:173–196. https://doi.org/10.1144/SP294.10
Muhlbauer JG, Fedo CM, Farmer GL (2017) Influence of textural parameters on detrital-zircon age spectra with application to provenance and paleogeography during the Ediacaran-Terreneuvian of southwestern Laurentia. GSA Bull 129(11–12):1585–1601. https://doi.org/10.1130/b31611.1
Mwiya S (2015) Environmental scoping report for the proposed petroleum exploration (satellite, airborne surveys, radiometric, geochemical, passive tellurics and finally drilling) for PEL 68 covering Blocks 2219 and 2319, Nama Basin, Omaheke Region, Onshore Eastern Namibia. PEP Rep 68:1–53
Naing TT, Bussien DA, Winkler WH, Nold M, von Quadt A (2014) Provenance study on Eocene–Miocene sandstones of the Rakhine Coastal Belt, Indo-Burman Ranges of Myanmar: geodynamic implications. Geol Soc London SP 386:195–216. https://doi.org/10.1144/SP386.10
Nasdala L, Zhang M, Kempe U, Panczer G, Gaft M, Andrut M, Plötze M (2003) Spectroscopic methods applied to zircon. In: Hanchar JM, Hoskin WO (eds) Zircon. Rev Min Geochem 53:427–467. https://doi.org/10.1515/9781501509322-018
Nash DJ, De Cort G, Chase BM, Verschuren D, Nicholson SE, Shanahan TM, Asrat A, Lézine A-M, Grab SW (2016) African hydroclimatic variability during the last 2000 years. Quat Sci Rev 154:1–22. https://doi.org/10.1016/j.quascirev.2016.10.012
Nickovic S, Cvetkovic B, Petković S, Amiridis V, Pejanović G, Solomos S, Marinou E, Nikolic J (2021) Cloud icing by mineral dust and impacts to aviation safety. Sci Rep 11:6411. https://doi.org/10.1038/s41598-021-85566-y
Nicoll K (2010) Geomorphic development and Middle Stone Age archaeology of the Lower Cunene River Namibia-Angola Border. Quat Sci Rev 29(11–12):1419–1431. https://doi.org/10.1016/j.quascirev.2009.02.026
Niemi NA (2013) Detrital zircon age distributions as a discriminator of tectonic versus fluvial transport: an example from the Death Valley, USA, extended terrane. Geosphere 9(1):126–137. https://doi.org/10.1130/GES00820.1
Nieminski NM, Grove M, Lowe DR (2019) Provenance of the Neoproterozoic deep-water Zerrissene Group of the Damara Orogen, Namibia, and paleogeographic implications for the closing of the Adamastor Ocean and assembly of the Gondwana supercontinent. GSA Bull 131(3/4):355–371. https://doi.org/10.1130/B32032.1
Oriolo S, Becker T (2018) The Kalahari Craton, Southern Africa: From Archean crustal evolution to Gondwana amalgamation. In: Siegesmund S, Basei MAS, Oyhatçabal P (eds) Geology of Southwest Gondwana. Regional Geol Rev 133–159. https://doi.org/10.1007/978-3-319-68920-3_6
Osorio-Granada E, Restrepo-Moreno SA, Muñoz-Valencia JA, Trejos-Tamayo RA, Pardo-Trujillo A, Barbosa-Espita AA (2017) Detrital zircon typology and U/Pb geochronology for the Miocene Ladrilleros–Juanchaco sedimentary sequence, Equatorial Pacific (Colombia): new constraints on provenance and paleogeography in northwestern South America. Geol Acta 15(3):201–215. https://doi.org/10.1344/GeologicaActa2017.15.3.4
Osorio-Granada E, Pardo-Trujillo A, Restrepo-Moreno SA, Gallego F, Muñoz J, Plata A, Trejos-Tamayo R, Vallejo F, Barbosa-Espita A, Cardona-Sánchez FJ, Foster DA, Kamenov G (2020) Provenance of Eocene-Oligocene sediments in the San Jacinto Fold Belt: paleogeographic and geodynamic implications for the northern Andes and the southern Caribbean. Geosphere 16(1):210–228. https://doi.org/10.1130/GES02059.1
Pearson DG, Scott JM, Liu J, Schaeffer A, Hongliang Wang L, van Hunen J, Szilas K, Chacko T, Kelemen PB (2021) Deep continental roots and cratons. Nature 596:199–210. https://doi.org/10.1038/s41586-021-03600-5
Peterson RG, Stramma L (1991) Upper-level circulation in the South Atlantic Ocean. Prog Oceanogr 26:1–73. https://doi.org/10.1016/0079-6611(91)90006-8
Pupin JP (1980) Zircon and granite petrology. Contrib Min Petrol 73:207–220. https://doi.org/10.1007/BF00381441
Rainbird RH, Hamilton MA, Yong GM (2001) Detrital zircon geochronology and provenance of the Torridonian, NW Scotland. J Geol Soc London 158:15–27. https://doi.org/10.1144/gsjgs.156.5.1021
Ribas F, Falqués A, van den Berg N, Cablleria M (2013) Modelling shoreline sand waves on the coasts of Namibia and Angola. Int J Sed Res 28:338–348. https://doi.org/10.1016/S1001-6279(13)60044-X
Ringrose S, Huntsman-Mapila P, Downey W, Coetzee S, Fey M, Vanderpost C, Vink B, Kemosidile T, Kolokose D (2008) Diagenesis in Okavango fan and adjacent dune deposits with implications for the record of palaeo-environmental change in Makgadikgadi–Okavango–Zambezi basin, northern Botswana. Geomorphology 101:544–557. https://doi.org/10.1016/j.geomorph.2008.02.008
Rino S, Kon Y, Sato W, Maruyama S, Santosh M, Zhao D (2008) The Grenvillian and Pan-African orogens: world's largest orogenies through geologic time, and their implications on the origin of superplume. Gondwana Res 14:51–72. https://doi.org/10.1016/j.gr.2008.01.001
Saalmann K, Mänttäri I, Nyakecho C, Isabirye E (2016) Age, tectonic evolution and origin of the Aswa Shear Zone in Uganda: activation of an oblique ramp during convergence in the East African Orogen. J Afr Earth Sci 117:303–330. https://doi.org/10.1016/j.jafrearsci.2016.02.002
Scherer E, Munker C, Mezger K (2001) Calibration of the Lutetium–Hafnium clock. Science 293(5530):683–687. https://doi.org/10.1126/science.1061372
Schmitt AK, Emmermann R, Trumbull RB, Bühn B, Henjes-Kunst F (2000) Petrogenesis and $^{40}Ar/^{39}Ar$ geochronology of the brandberg complex, Namibia: evidence for a major mantle contribution in metaluminous and peralkaline granites. J Petrol 41:1207–1239. https://doi.org/10.1093/petrology/41.8.1207
Seth B, Armstrong RA, Brandt S, Villa IM, Kramers JD (2003) Mesoproterozoic U-Pb and Pb-Pb ages of granulites in NW Namibia:

reconstructing a complete orogenic cycle. Precambrian Res 126:147–168. https://doi.org/10.1016/S0301-9268(03)00193-1
Seth B, Armstrong RA, Büttner A, Villa IM (2005) Time constraints for Mesoproterozoic upper amphibolite facies metamorphism in NW Namibia: a multi-isotopic approach. Earth Planet Sci Lett 230:355–378. https://doi.org/10.1016/j.epsl.2004.11.022
Shakeel A, Kirichek A, Chassagne C (2020) Rheological analysis of mud from Port of Hamburg, Germany. J Soils Sed 20:2553–2562. https://doi.org/10.1007/s11368-019-02448-7
Shi N, Schneider R, Beug H-J, Dupont LM (2001) Southeast trade wind variations during the last 135 kyr: evidence from pollen spectra in eastern South Atlantic sediments. Earth Planet Sci Lett 187:311–321. https://doi.org/10.1016/S0012-821X(01)00267-9
Sláma J, Košler J (2012) Effects of sampling and mineral separation on accuracy of detrital zircon studies. Geochem Geophys Geosys 13(5):Q05007. https://doi.org/10.1029/2012GC004106
Sláma J, Košler J, Condon DJ, Crowley JL, Gerdes A, Hanchar JM, Horstwood MSA, Morris GA, Nasdala L, Norberg N, Schaltegger U, Schoene B, Tubrett MN, Whitehouse MJ (2008) Plešovice zircon—a new natural reference material for U-Pb and Hf isotopic microanalysis. Chem Geol 249:1–35. https://doi.org/10.1016/j.chemgeo.2007.11.005
Spearman J, Manning AJ (2017) On the hindered settling of sand-mud suspensions. Ocean Dyn 67:465–483. https://doi.org/10.1007/s10236-017-1034-7
Spencer CJ, Kirkland CL, Taylor RJM (2016) Strategies towards statistically robust interpretation of in situ U-Pb zircon geochronology. Geosci Front 7:581–589. https://doi.org/10.1016/j.gsf.2015.11.006
Stacey JS, Kramers JD (1975) Approximation of terrestrial lead isotope evolution by a two-stage model. Earth Planet Sci Lett 26:207–221. https://doi.org/10.1016/0012-821X(75)90088-6
Stevens T, Palk C, Carter A, Lu H, Clift P (2010) Assessing the provenance of loess and desert sediments in northern China using U-Pb dating and morphology of detrital zircons. GSA Bull 122(7/8):1331–1344. https://doi.org/10.1130/B30102.1
Strohbach BJ (2008) Mapping the major catchments of Namibia. Agricola 18:63–73
Tack L, Wingate MTD, Liégeois J-P, Fernandez-Alonso M, Deblond A (2001) Early Neoproterozoic magmatism (1000–910 Ma) of the Zadinian and Mayumbian Groups (Bas-Congo): onset of Rodinia rifting at the western edge of the Congo craton. Precambrian Res 110:277–306. https://doi.org/10.1016/S0301-9268(01)00192-9
Tchameni R, Lerouge C, Penaye J, Cocherie A, Milesi JP, Toteu SF, Nsifa NE (2010) Mineralogical constraint for metamorphic conditions in a shear zone affecting the Archaean Ngoulemakong tonalite, Congo craton (Southern Cameroon) and retentivity of U-Pb SHRIMP zircon dates. J Afr Earth Sci 58:67–80. https://doi.org/10.1016/j.jafrearsci.2010.01.009
Thiéblemont D, Callec Y, Fernandez-Alonso M, Chène F (2018) A geological and isotopic framework of precambrian terrains in Western Central Africa: an introduction. In: Siegesmund S, Basei MAS, Oyhatçabal P (eds) Geology of Southwest Gondwana. Regional Geol Rev 107–132. https://doi.org/10.1007/978-3-319-68920-3_5
Thomas RJ, Spencer C, Bushi AM, Baglow N, Boniface N, de Kock G, Horstwood MSA, Hollick L, Jacobs J, Kajara S, Kamihanda G, Key RM, Maganga Z, Mbawala F, McCourt W, Momburi P, Moses F, Mruma A, Myambilwa Y, Roberts NMW, Saidi H, Nyanda P, Nyoka K, Millar I (2016) Geochronology of the central Tanzania Craton and its southern and eastern orogenic margins. Precambrian Res 277:47–67. https://doi.org/10.1016/j.precamres.2016.02.008
van der Lubbe HJL, Frank M, Tjallingii R, Schneider RR (2016) Neodymium isotope constraints on provenance, dispersal, and climate-driven supply of Zambezi sediments along the Mozambique Margin during the past ~ 45,000 years. Geochem Geophys Geosyst 17:181–198. https://doi.org/10.1002/2015GC006080
van Schijndel V, Cornell DH, Frei D, Simonsen SL, Whitehouse MJ (2014) Crustal evolution of the rehoboth Province from archaean to mesoproterozoic times: insights from the rehoboth basement Inlier. Precambrian Res 240:22–36. https://doi.org/10.1016/j.precamres.2013.10.014
van Niekerk HS (2006) The origin of the Kheis Terrane and its relationship with the Archaean Kaapvaal Craton and the Grenvillian Namaqua Province in southern Africa. PhD thesis, University of Johannesburg
van der Westhuizen A (2012) Provenance of alluvial diamonds in southern Africa: a morphological and mineral chemistry study of diamonds and related heavy minerals from the Vaal-Orange system and the west coast. Unpublished Doctoral Thesis, University of Stellenbosch
Vermeesch P (2013) Multi-sample comparison of detrital age distributions. Chem Geol 341:140–146. https://doi.org/10.1016/j.chemgeo.2013.01.010
Vermeesch P, Garzanti E (2015) Making geological sense of 'Big Data' in sedimentary provenance analysis. Chem Geol 409:20–27. https://doi.org/10.1016/j.chemgeo.2015.05.004
Vermeesch P, Fenton CR, Kober F, Wiggs GFS, Bristow CS, Xu S (2010) Sand residence times of one million years in the Namib Sand Sea from cosmogenic nuclides. Nat Geosci 3:862–865. https://doi.org/10.1038/ngeo985
Vermeesch P, Resentini A, Garzanti E (2016) An R package for statistical provenance analysis. Sedim Geol 336:14–26. https://doi.org/10.1016/j.sedgeo.2016.01.009
Villaros A, Buick IS, Stevens G (2012) Isotopic variations in S-type granites: an inheritance from a heterogeneous source? Contrib Mineral Petrol 163:243–257. https://doi.org/10.1007/s00410-011-0673-9
Villeneuve M, Gärtner A, Kalikone C, Wazi N, Hofmann M, Linnemann U (2019) U-Pb ages and provenance of detrital zircons from the metasedimentary rocks of the Nya-Ngezie and Bugarama groups (D.R. Congo): a key for the evolution of the Mesoproterozoic Kibaran–Burundian orogen in central Africa. Correlations with the Kivu, Karagwe–Ankolean and Kibaride belts and Geodynamic interpretations. Precambrian Res 328:81–98. https://doi.org/10.1016/j.precamres.2019.04.003
Walraven F, Rumvegeri BT (1993) Implications of whole-rock Pb-Pb and zircon evaporation dates for the early metamorphic history of the Kasaï craton, Southern Zaïre. J Afr Earth Sci 16:395–404. https://doi.org/10.1016/0899-5362(93)90098-B
Ward JD (1984) Aspects of the cenozoic geology in the kuiseb valley, central Namibian Desert. PhD thesis, University of Natal
Ward JD (1989) Aspects of the geomorphology of Sandwich Harbour, Walvis lagoon and the related coast. Excursion Guide. Geol Soc SWA/Namibia: 4
Ward JD, Bulley BG (1988) Aeolian deposits at Henties Bay, central Namib coast: provenance and engineering implications. Commun Geol Surv SW Afr/namibia 4:29–31
Wayne DM, Sinha AK (1988) Physical and chemical response of zircons to deformation. Contrib Mineral Petrol 98:109–121. https://doi.org/10.1007/BF00371915
Wedepohl PM, Lurjeharms JRE, Meeuwis JM (2000) Surface drift in the south-east Atlantic Ocean. S Afr J Mar Sci 22:71–79. https://doi.org/10.2989/025776100784125671
Westerhof ABP, Härmä P, Isabirye E, Katto E, Koistinen T, Kuosmanen E, Lehto T, Lehtonen MI, Mäkitie H, Manninen T, Mänttäri I, Pekkala Y, Pokki J, Saalmann K, Virransalo P (2014) Geology and geodynamic development of uganda with explanation of the 1:1,000,000 scale geological map. Geol Surv Finl SP 55:1–387

Wigand M, Schmitt AK, Trumbull RB, Villa IM, Emmermann R (2004) Short-lived magmatic activity in an anorogenic subvolcanic complex: $^{40}Ar/^{39}Ar$ and ion microprobe U-Pb zircon dating of the Erongo, Damaraland, Namibia. J Volcanol Geoth Res 130:285–305. https://doi.org/10.1016/S0377-0273(03)00310-X

Wilson AH, Zeh A (2018) U-Pb and Hf isotopes of detrital zircons from the Pongola Supergroup: constraints on deposition ages, provenance and Archean evolution of the Kaapvaal craton. Precambrian Res 305:177–196. https://doi.org/10.1016/j.precamres.2017.12.020

Zeh A, Gerdes A, Barton JM Jr (2009) Archean accretion and crustal evolution of the Kalahari Craton—the Zircon Age and Hf Isotope Record of Granitic Rocks from Barberton/Swaziland to the Francistown Arc. J Petrol 50:933–966. https://doi.org/10.1093/petrology/egp027

Zhang P, Najman Y, Mei L, Millar I, Sobel ER, Carter A, Barfod D, Dhuime B, Garzanti E, Govin G, Vezzoli G, Hu X (2019) Palaeodrainage evolution of the large Rivers of East Asia, and Himalayan-Tibet tectonics. Earth Sci Rev 192:601–630. https://doi.org/10.1016/j.earscirev.2019.02.003

Zieger J, Rothe J, Hofmann M, Gärtner A, Linnemann U (2019) The Permo-Carboniferous Dwyka Group of the Aranos Basin (Namibia)—how detrital zircons help understanding sedimentary recycling during a major Glaciation. J Afr Earth Sci 158:103555. https://doi.org/10.1016/j.jafrearsci.2019.103555

Zieger J, Harazim S, Hofmann M, Gärtner A, Gerdes A, Marko L, Linnemann U (2020a) Mesozoic deposits of SW Gondwana (Namibia)—Unraveling Gondwanan sedimentary dispersion drivers by detrital zircon. Int J Earth Sci 109:1683–1704. https://doi.org/10.1007/s00531-020-01864-2

Zieger J, Stutzriemer M, Hofmann M, Gärtner A, Gerdes A, Marko L, Linnemann U (2020b) The evolution of the southern Namibian Karoo-aged basins: implications from detrital zircon data. Int Geol Rev. https://doi.org/10.1080/00206814.2020.1795732

Zoleikhaei Y, Frei D, Morton A, Zamanzadeh SM (2016) Roundness of heavy minerals (zircon and apatite) as a provenance tool for unraveling recycling: a case study from the Sefidrud and Sarbaz rivers in N and SE Iran. Sed Geol 342:106–117. https://doi.org/10.1016/j.sedgeo.2016.06.016